INFRARED ABSORPTION IN DOPED SEMICONDUCTORS DUE TO DIRECT INTERSUBBAND TRANSITIONS

by

JEFFREY PAUL HEBB

B.Eng. Mechanical Engineering, Technical University of Nova Scotia (1991)

Submitted to the Department of Mechanical Engineering
in partial fulfillment of the requirements for the degree of

MASTER OF SCIENCE IN MECHANICAL ENGINEERING

at the

MASSACHUSETTS INSTITUTE OF TECHNOLOGY

February, 1993

© 1993 Massachusetts Institute of Technology
All rights reserved

Signature of Author_____
Department of Mechanical Engineering
February, 1993

Certified by_____
Professor Markus I. Flik
Department of Mechanical Engineering
Thesis Supervisor

Accepted by_____
Professor Ain A. Sonin
Department of Mechanical Engineering
Chairman, Graduate Committee

MASSACHUSETTS INSTITUTE
OF TECHNOLOGY
MAR 24 1993
ARCHIVES

INFRARED ABSORPTION IN DOPED SEMICONDUCTORS DUE TO DIRECT INTERSUBBAND TRANSITIONS

by

JEFFREY PAUL HEBB

Submitted to the Department of Mechanical Engineering
on February 2, 1993 in partial fulfillment of the requirements
for the Degree of Master of Science in Mechanical Engineering

ABSTRACT

This work proposes a simple, yet accurate model for infrared absorption due to direct intersubband transitions in doped semiconductors. Direct intersubband transitions are modeled as a continuum of semiclassical damped harmonic oscillators, with the resonant frequency of each oscillator in the continuum determined by the electronic band structure. The free-electron mass is replaced by an average effective mass which accounts for the interaction of the electron with the crystal lattice. The intersubband relaxation time and a quantum-mechanical parameter governing the transition probability are assumed to be independent of the electron wavevector, and are treated as adjustable parameters. The room-temperature absorptance spectra of p-type GaAs samples with dopant concentrations from 8×10^{17} to 1×10^{20} cm^{-3} are determined experimentally using a Fourier transform-infrared spectrometer in the infrared spectral region from 1 to 25 μm. The absorptance spectra are fitted using the proposed model, which provides the optical constants of p-type GaAs for the dopant concentrations of the samples, as well as expressions for the dopant-concentration dependence of the adjustable parameters. Potential applications of the model are semiconductor process control and infrared detector design.

Thesis Supervisor: Markus I. Flik
Title: Assistant Professor of Mechanical Engineering

To my father, Paul and to the
memory of my mother, Virginia

ACKNOWLEDGMENTS

I would like to thank my advisor, Professor Markus I. Flik, for his encouragement and enthusiastic guidance during the course of this research. Technical advice and moral support from Professor Ernest G. Cravalho is also appreciated. I am indebted to my colleagues Dr. Zhoumin Zhang, Ken Goodson, Mac Whale, Norman Christophersen, and Chris Bang for their technical support and friendship. Especially, I would like to thank Chris Malone for his faithful companionship and sense of humour, and Dr. Byung-In Choi for his calm wisdom and friendship.

I am also grateful, more than I am able to express in words, to my dear father Paul and to my wonderful sisters Catherine, Sharon, and Beverley for their love and support. Thanks also to my old friends in Halifax and my Cantabrigian friend, Elizabeth Temin, for providing timely breaks from my work.

Technical guidance from Professors Klavs F. Jensen and Adel F. Sarofim of the Department of Chemical Engineering, and Professor Lionel C. Kimerling of the Department of Materials Science and Engineering, is appreciated. Dr. William Hoke at Raytheon Company, Lexington, MA, and Paul Martin of Professor Clifton G. Fonstad's group kindly provided GaAs samples and technical advice. Financial support came from the Lynde and Harry Bradley Foundation.

TABLE OF CONTENTS

NOMENCLATURE

A_{fs} = near-normal spectral absorptance of a film-substrate composite

C_{ij} = square of the magnitude of the momentum matrix element, kg eV

d_f = film thickness, m

d_s = substrate thickness, m

E = electron energy, eV

E_F = Fermi energy, eV

E_G = band-gap energy, eV

E_l = electron energy for band l, eV

E_V = electron energy at the top of the valence band, eV

e = magnitude of the charge of an electron = 1.602×10^{-19} C

$F_{1/2}$ = Fermi-Dirac integral of order 1/2

F_{ext} = force on an electron in a crystal other than the lattice force, N

f_{ij} = oscillator strength for a transition in a solid from band i to band j

f_{mn} = oscillator strength for a transition in an atom from state m to state n.

h_p = Planck's constant divided by $2\pi = 1.0552 \times 10^{-34}$ J s

i = $\sqrt{-1}$

$\boldsymbol{k}$ = electron wavevector, m^{-1}

k = magnitude of the electron wavevector, m^{-1}

k_B = the Boltzmann constant = 1.381×10^{-23} J s^{-1}

M_{ij} = momentum matrix element for a transition from band i to band j, $(\text{kg eV})^{1/2}$

M_{mn} = momentum matrix element for a transition in an atom from state m to state n, $(\text{kg eV})^{1/2}$

m_{dos} = density-of-states effective mass, kg

m_{ij} = average dynamic effective mass, kg

m_l = dynamic effective mass of a carrier in band l, kg

m_o = free-electron mass = 9.11×10^{-31} kg

N = concentration of free carriers, m^{-3}

N_A = concentration of acceptor atoms, m^{-3}

N_V = effective density of valence band states, m^{-3}

n = refractive index

p = occupation probability at thermal equilibrium

R_{fs} = near-normal spectral reflectance of a film-substrate composite

$\boldsymbol{r}$ = position vector, m

T_{fs} = near-normal spectral transmittance of a film-substrate composite

T = temperature, K

t = time, s

v = velocity of electron wavepacket, m s^{-1}

Z = total number of electrons in an atom

Γ_{mn} = damping coefficient for an electronic transition in an atom, rad s^{-1}

γ_{ph} = optical-phonon damping coefficient, rad s^{-1}

Δ = spin-orbit splitting energy of GaAs = 0.34 eV

ΔA_{off} = spectral-overlap absorptance offset at a wavelength of 2.5 μm

ΔR_{off} = spectral-overlap reflectance offset at a wavelength of 2.5 μm

ε = dielectric function

ε_{fc} = contribution of free carriers to the dielectric function

ε_{ij} = contribution of intersubband transitions between band i and band j to the dielectric function

ε_{isb} = contribution of all intersubband transitions to the dielectric function

ε_o = electrical permittivity of free space = 8.854×10^{-12} C V^{-1} m^{-1}

ε_{ph} = contribution of optical phonons to the dielectric function

κ	=	extinction coefficient
λ	=	wavelength of radiation in vacuum, m
μ	=	free-carrier mobility, $m^2\ V^{-1}\ s^{-1}$
ρ	=	density of states in k-space, m^{-2}
τ_{fc}	=	intrasubband (free-carrier) relaxation time, s
τ_{ij}	=	intersubband relaxation time for a transition from band i to band j, s
τ_{mn}	=	relaxation time for a transition in an atom, s
χ^2	=	chi-squared merit function
ω	=	photon frequency, rad s^{-1}
ω_{ij}	=	transition frequency for a transition from band i to band j, rad s^{-1}
ω_L	=	longitudinal optical phonon frequency, rad s^{-1}
ω_{mn}	=	transition frequency for a transition in an atom, rad s^{-1}
ω_p	=	plasma frequency, rad s^{-1}
ω_T	=	transverse optical phonon frequency, rad s^{-1}
ψ	=	wave function of an electron in an atom or a solid

Subscripts

1	=	heavy-hole band
2	=	light-hole band
3	=	split-off band
a	=	atom
e	=	electron
f	=	film
h	=	hole
i	=	index of the energy band containing the initial state of a transition
j	=	index of the energy band containing the final state of a transition

l	=	band index
m	=	initial state of electron for an atomic transition
n	=	final state of an electron for an atomic transition
s	=	substrate

LIST OF FIGURES

LIST OF TABLES

1. INTRODUCTION

Doped semiconductors play a crucial role in electronic and optical devices such as transistors and infrared detectors. Knowledge of the infrared optical constants of doped semiconductors is required for the thermal modeling of semiconductor deposition processes, optical techniques for *in situ* process control, and optical device design. The available data for the optical constants of doped semiconductors do not cover the wide spectral and dopant-concentration range that is required to achieve these tasks.

For wavelengths greater than the band-gap wavelength of doped semiconductors, radiation is absorbed through intrasubband transitions (free-carrier absorption), intersubband transitions, and optical phonons. The effects of all of these absorption mechanisms on the optical constants can be described using quantum-mechanical models (Wooten, 1972), but absorption by optical phonons and free carriers is often modeled using simple classical or semiclassical models (Perkowitz, 1992). Absorption by optical phonons can be modeled with the classical Lorentz model, and free-carrier absorption can been modeled with the semiclassical Drude model. These models are useful for engineering calculations because they are computationally efficient, and they contain physically meaningful adjustable parameters that allow the achievement of quantitative agreement with experimental data. This work develops a simple model of this type for *direct* intersubband transitions, which are transitions for which the wavevector of the electron is unchanged.

The most commonly used quantum-mechanical formulation for calculating the contribution to the dielectric function of direct band-to-band transitions, described by Bassani and Parravicini (1975), directly relates the optical constants to the band structure of the solid. These calculations are generally complicated and lengthy, and agreement with experimental data is often poor. The predicted reflectance spectra of semiconductors such as Si and GaAs typically differ by 10 to 15 percent from the measured reflectance in the

visible and ultraviolet spectral regions (Cohen and Chelikowsky, 1989). Kane (1956) used this method to calculate the infrared absorption coefficient due to direct intersubband transitions for p-type Ge. The qualitative features of the experimental data were predicted, but quantitative agreement was not achieved. Huberman et al. (1991) calculated the optical constants of heavily doped p-type GaAs considering direct intersubband transitions using the method of Kane (1956) and the damped harmonic oscillator model. The calculated absorptance of thin-film samples agreed qualitatively with experimental data throughout most of the spectrum, but there was a difference in magnitude of as much as 30 percent throughout significant portions of the spectrum.

Simpler methods of calculating the effects of interband transitions are more empirical and involve many adjustable parameters. Verleur (1968) successfully fitted the reflectance of several solids in spectral regions dominated by interband transitions by using a collection of damped harmonic oscillators. This method used many adjustable parameters (e.g., 22 adjustable parameters to fit the reflectance spectrum of Si), none of which had physical meaning. Forouhi and Bloomer (1992) proposed a method of determining optical constants that considered each peak in the reflectance spectrum of a solid to be the result of a transition between two quantum-mechanical states. The assumption of a finite lifetime of the excited state yielded expressions for the optical constants. Quantitative agreement with measured data was achieved for the optical constants of a variety of solids, but many adjustable parameters were required to achieve this fitting (e.g., 14 adjustable parameters to fit the reflectance spectrum of Si) and *a priori* knowledge of the spectrum was required to obtain good initial guesses for the adjustable parameters. The main disadvantage of using these models for intersubband transitions in doped semiconductors is the difficulty in the interpolation or extrapolation of the adjustable parameters to dopant concentrations which have not been investigated experimentally.

The present work proposes a simple, yet accurate model for absorption due to direct intersubband transitions in doped semiconductors. Direct intersubband transitions are

modeled as a continuum of semiclassical damped harmonic oscillators, with the resonant frequency of each oscillator in the continuum determined by the electronic band structure. The free-electron mass is replaced by an average effective mass which accounts for the interaction of the electron with the crystal lattice. The intersubband relaxation time and a quantum-mechanical parameter governing the transition probability are assumed to be independent of the electron wavevector, and are treated as adjustable parameters. The room-temperature absorptance spectra of p-type GaAs samples with dopant concentrations from 8×10^{17} to 1×10^{20} cm^{-3} are determined experimentally using a Fourier transform-infrared (FT-IR) spectrometer in the infrared spectral region from 1 to 25 μm. The absorptance spectra are fitted using the proposed model, which provides the optical constants of p-type GaAs for the dopant concentrations of the samples, as well as expressions for the dopant-concentration dependence of the adjustable parameters.

The extension of this model to other p-type semiconductors and to higher temperatures may facilitate tools for the control of deposition processes such as adaptively calibrated pyrometry (Choi et al., 1992a) and *in situ* FT-IR spectroscopy (Choi et al., 1993). This model could also be useful for the analysis and design of infrared detectors which exploit intersubband transitions, such as heterojunction internal photoemission detectors (Huberman et al., 1991) and $GaAs/Al_xGa_{1-x}As$ multiple quantum well detectors (Osbourn, 1990).

2. SEMICONDUCTOR BAND STRUCTURES AND TRANSITIONS

2.1 Energy Bands and the Semiclassical Equations of Motion

An electronic state in an isolated atom is characterized by a wave function, $\psi_a(\mathbf{r})$, with an associated energy E, where $\boldsymbol{r}$ is a position vector in real space. The energies of atomic states are discrete, and the wave functions are localized in space. When atoms are brought together to form a solid, the atomic wave functions interact such that the states form a quasi-continuous set of energy bands and the valence electrons are mobile in the periodic potential created by the crystal lattice (Harrison, 1980). Each electronic state is represented by a wave function $\psi_l(\boldsymbol{k})$, with an associated energy, $E_l(\boldsymbol{k})$, where l is the band index and $\boldsymbol{k}$ is the wavevector. The function $E_l(\boldsymbol{k})$ is referred to as the *electronic band structure* of the solid. The band structure for a typical semiconductor, GaAs, is shown in Fig. 2-1. The energy bands are arranged into two groups, the *valence band* and the *conduction band*, which are separated by an energy gap, E_G, and consist of energy subbands. In Fig. 2-1, $E(k)$ is shown for one direction in $\boldsymbol{k}$-space, where k is the magnitude of the wavevector $\boldsymbol{k}$. Here, the conduction subband is calculated by assuming that E is proportional to k^2 for illustrative purposes, and the valence subbands are calculated by fitting a polynomial function to the results of band-structure calculations performed by Huberman et al. (1991), which are explained in greater detail in Chapter 4.

Although band structures are usually displayed as continuous curves, they are actually a set of closely-spaced discrete points in $\boldsymbol{k}$-space. The origin of this discreteness of electronic states is the application of periodic boundary conditions to the wave-function solutions of the Schrödinger equation (Pierret, 1987). The closeness of the spacing of these states in an incremental interval of energy or an incremental volume of $\boldsymbol{k}$-space is

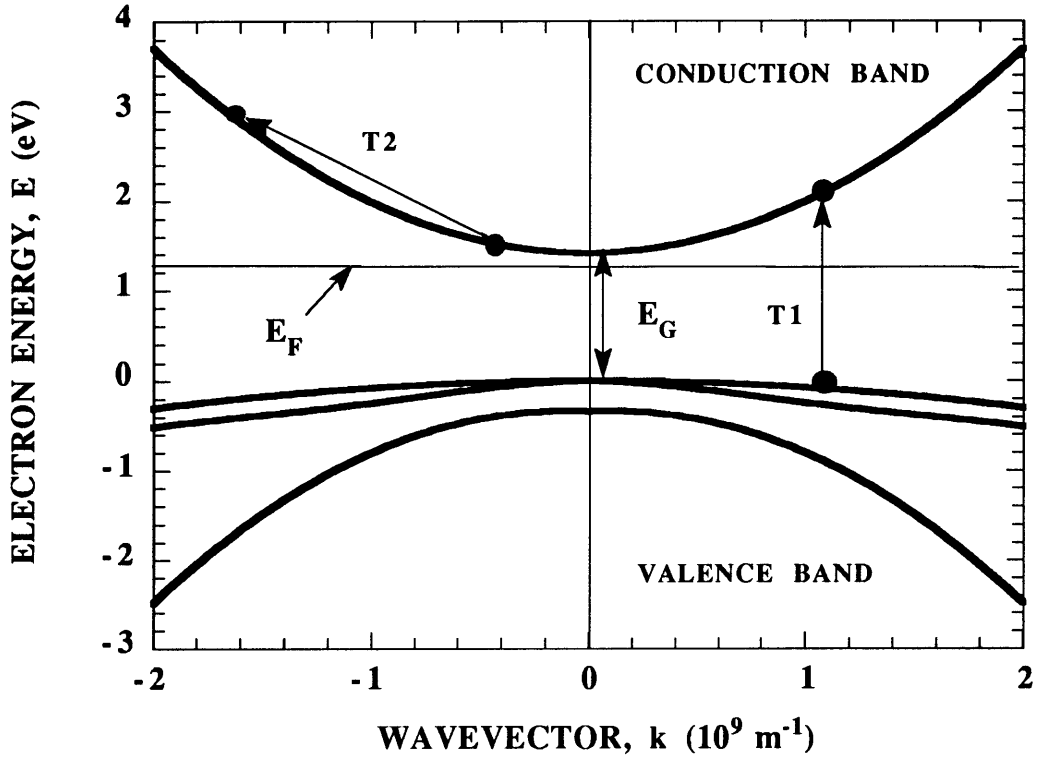

Figure 2-1 Band structure of GaAs. The Fermi energy is for n-type doping, (T1) is a direct interband transition, and (T2) is an intrasubband transition.

quantified by the electron density of states. A sum over the discrete electronic states is well approximated by an integral using the electron density of states (Kittel, 1986).

Once the band structure of a semiconductor is known, it can be used in conjunction with the semiclassical equations of motion to simply describe the dynamics of an electron in an applied electric field. In the semiclassical formulation, an electron in a state $E_l(\boldsymbol{k})$ is represented by a wavepacket consisting of a linear combination of wave functions having a distribution of wavevectors closely grouped around a peak wavevector, $\boldsymbol{k}$ (Harrison, 1980). This formulation assumes that the spatial variation of the applied field has a lengthscale much longer than the lattice constant, which is typically on the order of 5 Å. For a band structure that is isotropic in $\boldsymbol{k}$-space, the semiclassical equations of motion for this wavepacket are

$$v_l(k) = \frac{1}{h_p}\frac{dE_l(k)}{dk} \tag{1}$$

$$F_{ext} = \frac{d}{dt}(h_p k) = \left(\frac{1}{h_p^2}\frac{d^2E_l(k)}{dk^2}\right)^{-1}\frac{dv_l(k)}{dt} \tag{2}$$

$$m_l(k) = \left(\frac{1}{h_p^2}\frac{d^2E_l(k)}{dk^2}\right)^{-1} \tag{3}$$

where v_l is the group velocity of the wavepacket, F_{ext} is the external force acting on the electron not due to interaction with the crystal lattice, t is time, $h_p = 1.0552 \times 10^{-34}$ J s is Planck's constant divided by 2π, and m_l is the dynamic effective mass of the electron. Equation (2) resembles Newton's second law, with the mass of the free electron being replaced by a dynamic effective mass which is inversely proportional to the curvature of $E_l(k)$. The quantity $h_p k$ is referred to as the *crystal momentum* because of the similarity of Eq. (2) to Newton's second law.

The charge carriers in semiconductors are electrons and holes. The thermal excitation of an electron from the valence band to the conduction band leaves a vacancy in the valence band. This vacancy is conceptualized as a fictitious particle called a hole, which has a positive charge, e, where e is the magnitude of the charge of the electron. For a hole created by exciting an electron from the valence band with wavevector $\boldsymbol{k}$, energy E, effective mass m_e, and group velocity v, the wavevector, energy, effective mass, and group velocity are defined as $\boldsymbol{k}_h = -\boldsymbol{k}$, $E_h = -E$, $m_h = -m_e$, and $v_h = v$, respectively. Conventionally, the energy and wavevector of electrons are used, even if the carriers are holes.

2.2 Equilibrium Distribution of Carriers

The band structure contains information about the available electronic states in a solid, but does not contain any information concerning the occupation of these states by electrons. For the calculation of optical properties of semiconductors, it is necessary to determine the occupation probability for a particular state when the crystal is in thermal equilibrium. To determine the energy-dependent occupation probability, it is necessary to know the Fermi energy, E_F, and the temperature, T.

For an intrinsic (pure) semiconductor at zero temperature, the valence band is filled with electrons, the conduction band is empty, and E_F is approximately in the center of the band gap. At finite temperatures, free electrons are created by thermal excitation of electrons into the conduction band, which also creates free holes in the valence band. Free carriers can also be created by doping, which is the intentional introduction of impurities into an intrinsic semiconductor. Dopant atoms are introduced into the crystal which either donate a free electron or a free hole to the crystal. Donor dopant atoms donate an electron to the crystal, and the semiconductor is referred to as *n-type*. Acceptor dopant atoms accept an electron from the crystal, leaving a hole, and the semiconductor is referred to as *p-type*.

For n-type semiconductors, the donated electrons distribute themselves in the conduction band, and the Fermi energy increases (see Fig. 2-1). For p-type doping, the donated holes distribute themselves in the valence band, and the Fermi energy decreases. For p-type semiconductors, which are the focus of this work, the equations used to determine the Fermi level are (Pierret, 1987)

$$N = N_V \frac{2}{\sqrt{\pi}} F_{1/2}\left(\frac{E_V - E_F}{k_B T}\right) \tag{4}$$

$$N_V = 2 \left[\frac{2\pi m_{dos} k_B T}{(2\pi h_p)^2} \right]^{3/2} \tag{5}$$

$$m_{dos} = [(m_1)^{3/2} + (m_2)^{3/2}]^{2/3} \tag{6}$$

$$F_{1/2}(\eta) = \int_0^{\infty} \frac{\xi^{1/2}}{1 + \exp(\xi - \eta)} d\xi \tag{7}$$

where N is the concentration of free holes in the crystal, N_V is the effective density of valence band states, E_V is the energy of the uppermost valence subband at $k = 0$, $F_{1/2}$ is the Fermi-Dirac integral of order 1/2, m_{dos} is the density-of-states effective mass, $k_B = 1.381 \times 10^{-23}$ J s^{-1} is the Boltzmann constant, T is the temperature of the crystal, and m_1 and m_2 are the dynamic effective masses of the two uppermost valence subbands, the heavy- and light-hole bands, respectively, at $k = 0$. Once the Fermi energy is determined, the probabilities of an electron or a hole occupying a state of energy E are given by (Kittel, 1986)

$$p_e(E) = \frac{1}{1 + \exp\left(\frac{E - E_F}{k_B T}\right)} \tag{8}$$

$$p_h(E) = 1 - p_e(E) \tag{9}$$

where p_e and p_h are the occupation probabilities for electrons and holes, respectively.

2.3 Photon Absorption

Photons incident on a solid can be absorbed through the transition of an electron from a state of lower energy to a state of higher energy. The conditions that must be met for the occurrence of a photon-induced electronic transition from $E_i(\boldsymbol{k})$ to $E_j(\boldsymbol{k'})$ are (Ashcroft and Mermin, 1976) : (a) before the transition, the initial state must be occupied and the final state must be empty, (b) the crystal momentum plus the momentum of the other participating particles must be conserved, and (c) the total energy of the participating particles must be conserved.

An *interband* transition refers to a transition between an initial state in the conduction band and a final state in the valence band. An *intersubband* transition refers to a transition between subbands of the valence band or between subbands of the conduction band. An *intrasubband* transition refers to a transition within one subband of the conduction band or the valence band. A *direct* transition refers to a transition for which the wavevector of the electron is the same for the initial and final states, i.e., a vertical transition in the $E(\boldsymbol{k})$ diagram. Since the wavevector of a photon is much smaller than a typical wavevector of an electron, momentum conservation requires that a transition involving only a photon and an electron appears as a vertical transition on the $E(\boldsymbol{k})$ diagram. An *indirect* transition refers to a transition for which the wavevector of the electron in the initial state is significantly different from the wavevector of the final state. Interaction with another particle such as a phonon is required to satisfy momentum conservation.

Absorption of photons by direct and indirect interband transitions occurs in all semiconductors for photon energies greater than the band-gap energy, E_G. Since the band-gap energy of most semiconductors is of the order of 1 eV, absorption by interband transitions typically occurs at wavelengths shorter than approximately 1 μm. A direct interband transition labeled T1 is shown in Fig. 2-1. Absorption by intersubband and intrasubband transitions is only observed in doped semiconductors, because the subbands for undoped semiconductors are almost completely full or empty, and condition (a) is usually not satisfied. Intersubband absorption is observed for many n- and p-type semiconductors, typically in the spectral region between 1 and 10 μm (Fan, 1967). Intrasubband absorption, also referred to as free-carrier absorption, is observed for all doped semiconductors, and all transitions are necessarily indirect. Free-carrier absorption becomes stronger with increasing wavelength. An intrasubband transition for an n-type semiconductor, labeled T2, is shown in Fig. 2-1. An upward transition of an electron on the $E(\boldsymbol{k})$ diagram can also be treated as a downward transition of a hole, a common approach when considering intersubband and intrasubband transitions in p-type semiconductors.

3. THEORY OF DIRECT INTERSUBBAND TRANSITIONS

3.1 Electronic Transitions in an Atom

For a photon-induced transition of a single electron in an isolated atom between a state of energy E_m and a state of higher energy E_n, the contribution to the dielectric function is given by (Wooten, 1972)

$$\varepsilon_{mn}(\omega) = f_{mn} \frac{e^2}{m_o \varepsilon_o} \frac{1}{\omega_{mn}^2 - \omega^2 - i \Gamma_{mn} \omega} \tag{10}$$

where ω_{mn} is the resonant frequency of the transition, ω is the frequency of the incident photon, m_o is the free-electron mass, ε_o is electrical permittivity of free space, f_{mn} is the dimensionless oscillator strength, and Γ_{mn} is the damping coefficient for the transition. The resonant frequency and oscillator strength are given by

$$\omega_{mn} = \frac{E_n - E_m}{h_p} \tag{11}$$

$$f_{mn} = \frac{2 |M_{mn}|^2}{m_o h_p \omega_{mn}} \tag{12}$$

where M_{mn} is the momentum matrix element between states m and n, given by

$$M_{mn} = \int_{0 < |r| < \infty} \psi_m^*(r) \left(\frac{h_p}{i} \nabla_r \right) \psi_n(r) \, dr \tag{13}$$

where ψ_m^* is the complex conjugate of the wave function of state m, ψ_n is the wave function of state n, and $i = \sqrt{-1}$. The magnitude of M_{mn} indicates the strength of the coupling between the initial and final states in the presence of a radiation field. Equation (10) is obtained by solving the Schrödinger equation for an electron in an atom initially in state m, with the effect of the incident photon modeled as a first order time-dependent perturbation (Wooten, 1972). The damping coefficient is introduced as a mechanism to account for energy loss and is associated with a characteristic relaxation time, $\tau_{mn} = 1/\Gamma_{mn}$ (Garbuny, 1965).

The form of the dielectric function for a transition between two atomic energy levels is very similar to that of a classical Lorentz damped harmonic oscillator. The only difference is the presence of the dimensionless oscillator strength, f_{mn}. If a photon of frequency ω_{mn} is incident on an atom, f_{mn} is a measure of the probability of the occurrence of a transition from state m to state n. If one considers all the possible transitions in an atom from a state m which is filled with an electron to a state n which is empty, there is a sum rule for the oscillator strengths (Wooten, 1972),

$$\sum f_{mn} = Z \tag{14}$$

where Z is the total number of electrons in the system.

3.2 Direct Intersubband Transitions

A simple model of a solid can be constructed by considering electronic transitions in an atom. An isolated atom can be thought of as a set of discrete oscillators, with the resonant frequency of each oscillator being determined by the electronic energy levels in the atom (Garbuny, 1965). When the atoms are brought together to form a solid, the discrete oscillator frequencies form a continuum of oscillator frequencies which are determined by

the band structure. Wooten (1972) used this model to estimate the high-frequency dielectric constant of Si to within 25 percent of the measured value.

In the present work, a modified form of Eq. (10) is used to model direct intersubband transitions. For a single direct transition between a state $E_i(\boldsymbol{k})$ and a higher-energy state $E_j(\boldsymbol{k})$, the contribution to the dielectric function is assumed to be

$$\varepsilon_{ij}(\omega,\boldsymbol{k}) = f_{ij}(\boldsymbol{k}) \frac{e^2}{m_{ij}(\boldsymbol{k})\,\varepsilon_o} \frac{1}{\omega_{ij}^2(\boldsymbol{k}) - \omega^2 - i\frac{\omega}{\tau_{ij}(\boldsymbol{k})}} \tag{15}$$

where f_{ij} is the oscillator strength, m_{ij} is the average dynamic effective mass of the two states, ω_{ij} is the resonant frequency of the transition, and τ_{ij} is the intersubband relaxation time. The resonant frequency is given by

$$\omega_{ij}(\boldsymbol{k}) = \frac{E_j(\boldsymbol{k}) - E_i(\boldsymbol{k})}{h_p} \tag{16}$$

and the average dynamic effective mass is assumed to be

$$m_{ij}(\boldsymbol{k}) = \frac{m_i(\boldsymbol{k}) + m_j(\boldsymbol{k})}{2} \tag{17}$$

where $m_i(\boldsymbol{k})$ and $m_j(\boldsymbol{k})$ are the dynamic effective masses of the initial and final states, respectively.

The oscillator strength for a transition in an atom must be modified for application to a solid. The occupation probabilities of the initial and final states must be accounted for, and the wave functions of the atomic states must be replaced by the wave functions of the electronic states in the solid (Stern, 1963). To be consistent with the use of the average effective mass used in Eq. (15), the free-electron mass in Eq. (12) is also replaced by the

average effective mass, m_{ij}. Considering these modifications, the oscillator strength becomes

$$f_{ij}(\boldsymbol{k}) = \frac{2|M_{ij}(\boldsymbol{k})|^2}{m_{ij}\, h_p\, \omega_{ij}(\boldsymbol{k})} \{p_e[E_i(\boldsymbol{k})] - p_e[E_j(\boldsymbol{k})]\} \tag{18}$$

where p_e is calculated using Eq. (8), and the momentum matrix element M_{ij} is

$$M_{ij}(\boldsymbol{k}) = \int_{0<|\boldsymbol{r}|<\infty} \psi_i^*(\boldsymbol{k},\boldsymbol{r}) \left(\frac{h_p}{i}\nabla_r\right) \psi_j(\boldsymbol{k},\boldsymbol{r})\, d\boldsymbol{r} \tag{19}$$

where ψ_i^* is the complex conjugate of the wave function of the initial state and ψ_j is the wave function of the final state.

The replacement of the free electron mass in Eq. (10) by the average dynamic effective mass in Eq. (15) accounts for interaction of the electron with the crystal lattice in an approximate way through the semiclassical equations of motion. The use of an effective mass in the semiclassical Drude model is common practice, and here this approach is extended to intersubband transitions. It is postulated that this semiclassical correction to the oscillator mass will allow the transitions between a group of subbands at a particular wavevector to be modeled as transitions between energy levels of an atom. The sum rule, Eq. (14), may be approximately satisfied if f_{mn} is replaced by f_{ij}, and Z is replaced by the sum of the occupation probabilities calculated using Eq. (8).

To apply Eq.(15) to transitions between two bands in a solid, it is necessary to sum the contributions from all possible transitions. The contribution to the dielectric function of intersubband transitions from band i to band j is

$$\varepsilon_{ij}(\omega) = \sum_{\substack{allowed \\ \boldsymbol{k}}} f_{ij}(\boldsymbol{k}) \frac{e^2}{m_{ij}(\boldsymbol{k})\,\varepsilon_o} \frac{1}{\omega_{ij}^2(\boldsymbol{k}) - \omega^2 - i\frac{\omega}{\tau_{ij}(\boldsymbol{k})}} \tag{20}$$

where the allowed $\boldsymbol{k}$ are those discrete wavevectors for which electronic states exist, as discussed in Chapter 2. Equation (20) can be converted to an integral by introducing the density of states in $\boldsymbol{k}$-space, which is independent of the direction of $\boldsymbol{k}$ (Pierret, 1987). If the band structure is assumed to be isotropic in $\boldsymbol{k}$-space, then Eq. (20) can be integrated with respect to k, the magnitude of the wavevector. The validity of this assumption must be assessed for the particular semiconductor band structure being considered, but semiconductor energy bands generally show similar trends for different directions in $\boldsymbol{k}$-space for the regions of the band structure for which intersubband transitions occur. If the integration is performed with respect to k, the correct density of states is the number of states per unit volume that exist between two spherical shells in $\boldsymbol{k}$-space, one with radius k, the other with radius $k + dk$, given by $\rho(k) = k^2/\pi^2$ (Pierret, 1987). Introducing $\rho(k)$ and the assumption of isotropic energy bands into Eq. (20) yields the final result for direct intersubband transitions,

$$\varepsilon_{ij}(\omega) = \int_0^\infty f_{ij}(k) \frac{k^2}{\pi^2} \frac{e^2}{m_{ij}(k)\,\varepsilon_o} \frac{1}{\omega_{ij}^2(k) - \omega^2 - i\frac{\omega}{\tau_{ij}(k)}}\, dk \tag{21}$$

To determine the total contribution of intersubband transitions to the dielectric function, it is necessary to sum over all the pairs of bands between which transitions take place.

It is common in solids state physics to model direct transitions in a solid using the damped harmonic oscillator model. In the standard quantum-mechanical approach, transitions are assumed to have an infinite lifetime, so a transition at a particular frequency is represented by a delta function (Bassani and Parravicini, 1975). A finite lifetime can be accounted for by replacing the delta function by a Lorentzian function which is derived

from the damped harmonic oscillator model (Hodgson, 1970). Huberman et al (1991). used this approach to model intersubband transitions in p-type GaAs. This yielded an expression for the frequency-dependent conductivity which is equivalent to Eq. (21), except for the use of an average dynamic effective mass, m_{ij}, introduced in the present work.

4. DIELECTRIC FUNCTION OF P-TYPE SEMICONDUCTORS

4.1 Dielectric Function of Doped Semiconductors

The mechanisms of absorption in doped semiconductors for photon energies smaller than the band-gap energy are intersubband transitions, free-carrier absorption, and optical phonons. The dielectric function of doped semiconductors is a superposition of the contributions from each of these mechanisms,

$$\varepsilon(\omega) = (n + i\kappa)^2 = \varepsilon_\infty + \varepsilon_{fc}(\omega) + \varepsilon_{ph}(\omega) + \varepsilon_{isb}(\omega) \qquad (22)$$

where ε is the total dielectric function, n is the refractive index, κ is the extinction coefficient, ε_∞ is the high-frequency dielectric constant, ε_{fc} is the contribution of free-carrier absorption, ε_{ph} is the contribution of optical phonons, and ε_{isb} is the contribution of intersubband transitions. Each of these terms will now be discussed for p-type semiconductors, for which intersubband transitions are direct (Pankove, 1971). Particular consideration is given to p-type GaAs because it is the subject of the experimental investigation discussed in Chapter 5.

The high-frequency dielectric constant is dependent on the absorption that occurs at photon energies greater than the band-gap energy, which is due to interband transitions. In general, ε_∞ is dependent on dopant concentration because doping slightly changes the band structure and the occupation of available electron states. However, the effect of doping on ε_∞ is small, as shown by the measurements of the refractive index of p-type GaAs performed by Sell et al. (1974). They showed that $n = 3.49$ for undoped GaAs at a wavelength of 1.0 μm, compared to $n = 3.47$ for p-type GaAs with a dopant concentration of 1.5×10^{19} cm^{-3}. This change in refractive index corresponds to a change in ε_∞ of

approximately 0.1, which is of the order of the disagreement in the literature for the experimental value of ε_∞ for undoped GaAs (Blakemore, 1983). It is assumed in this work that $\varepsilon_\infty = 11.0$ (Palik, 1985) for all dopant concentrations.

The contribution of free-carrier absorption to the dielectric function is typically modeled using the semiclassical Drude theory (Perkowitz, 1992). The contribution from carriers in a partially-filled subband l is given by

$$\varepsilon_{fc}(\omega) = -\frac{\omega_p^2}{\omega^2 + i\frac{\omega}{\tau_{fc}}} = -\frac{\frac{N_l e^2}{m_l \varepsilon_o}}{\omega^2 + i\frac{\omega}{\tau_{fc}}} \tag{23}$$

where ω_p is the plasma frequency, N_l is the concentration of free carriers in the subband, m_l is the effective mass of the free carriers in the subband, and τ_{fc} is the intrasubband relaxation time of an excited carrier. For photon energies much smaller than the free-carrier energy, the equivalence of the semiclassical and quantum mechanical treatments of free-carrier absorption has been shown theoretically by Dumke (1967). This has been confirmed through successful fits of experimental data in the mid- and far-infrared spectral regions using the semiclassical Drude model (Perkowitz, 1992).

The relaxation time is governed by scattering of the free carriers on phonons, ionized dopant sites, and other free carriers, and can be estimated from experimental mobility by (Rode, 1975)

$$\tau_{fc} = \frac{\mu m_l}{e} \tag{24}$$

where μ is the mobility of the free carriers. For p-type GaAs, approximately 90 percent of the holes that result from acceptor doping are distributed in the heavy-hole band (Blakemore, 1983). In the present work, it is assumed that all holes reside in the heavy-hole band. The dynamic effective mass of heavy-holes at $\boldsymbol{k} = 0$, $m_l = 0.5\, m_o$

(Blakemore, 1983), is used in Eqs (23) and (24). It is also assumed that at room temperature, all dopant sites are ionized (Pierret, 1987) so that $N_I = N_A$, where N_A is the concentration of acceptor atoms in the crystal.

The contribution of optical phonons to the dielectric function of semiconductors can be approximated by (Palik , 1985)

$$\varepsilon_{ph}(\omega) = \frac{\varepsilon_\infty [(\omega_L)^2 - (\omega_T)^2]}{(\omega_T)^2 - \omega^2 - i\,\gamma_{ph}\,\omega} \tag{25}$$

where ω_L and ω_T are the longitudinal and transverse phonon frequencies, respectively, and γ_{ph} is the damping coefficient. Although there is some dependence of the phonon parameters on dopant concentration, this dependence is commonly ignored because at high doping levels, free-carrier absorption is dominant in the spectral regions of the phonon frequencies. For GaAs at room temperature, Palik (1985) averaged the best-fit parameters from several investigators to obtain recommended values of $\omega_L = 292.1$ cm^{-1}, $\omega_T = 268.7$ cm^{-1}, and $\gamma_{ph} = 2.4$ cm^{-1}. In the present work, these parameters are assumed to be independent of dopant concentration

4.2 Intersubband Transitions

In general, intersubband transitions in doped semiconductors may be direct or indirect, depending on the shape of the subbands participating in the transitions. Indirect transitions are generally less probable than direct transitions, and so their effects are usually only observed in spectral regions where there are no direct transitions (Hodgson, 1970). For n-type semiconductors, intersubband transitions occur between the conduction subbands, and can be direct or indirect transitions, depending on the particular semiconductor being considered. For p-type semiconductors, intersubband transitions

occur between the valence subbands and are considered to be direct transitions (Pankove, 1971). For this reason, the present work is concerned mainly with p-type semiconductors, although Eq. (21) is equally applicable to direct intersubband transitions in n-type semiconductors.

The first three valence subbands of GaAs are shown in Fig. 4-1. The heavy-hole band is assigned a band index of $l = 1$, the light-hole band $l = 2$, and the split-off band $l = 3$. The first three valence bands of most semiconductors are very similar to those of GaAs (Cohen and Chelikowsky, 1989). Equation (21) is written for transitions of electrons, but for p-type semiconductors it is more convenient to consider the transitions of holes. In this case, the oscillator frequency should be calculated by $\omega_{ij} = [E_i(k)-E_j(k)] / h_p$ instead of Eq. (16), since holes move downward on the $E(\boldsymbol{k})$ diagram when they absorb energy. The effective mass of the holes should be used to calculate m_{ij}, and the occupation probability of holes, p_h, should be used instead of p_e in Eq. (18). Summing over the possible transitions between the first three valence subbands yields

$$\varepsilon_{isb}(\omega) = \sum_{\substack{ij=12 \\ ij=13 \\ ij=23}} \int_0^\infty f_{ij}(k) \frac{k^2}{\pi^2} \frac{e^2}{m_{ij}(k)\,\varepsilon_o} \frac{1}{\omega_{ij}^2(k) - \omega^2 - i\frac{\omega}{\tau_{ij}(k)}}\, dk \qquad (26)$$

The summation in Eq. (26) considers direct transitions of holes from the heavy-hole band to the light-hole band ($ij = 12$), heavy-hole band to split-off band ($ij = 13$), and light-hole band to split-off band ($ij = 23$), as shown in Fig. 4-1. For the particular semiconductor being considered, it can be determined from experiment which transitions will have an observable effect on the radiative properties. For example, the effects of all three transitions have been observed in GaAs (Fan, 1967) and Ge (Kane, 1956), but only the transitions $ij = 12$ have been observed for InAs and GaSb (Fan, 1967). For InAs and GaSb, transitions to the split-off band occur at photon energies greater than the band-gap

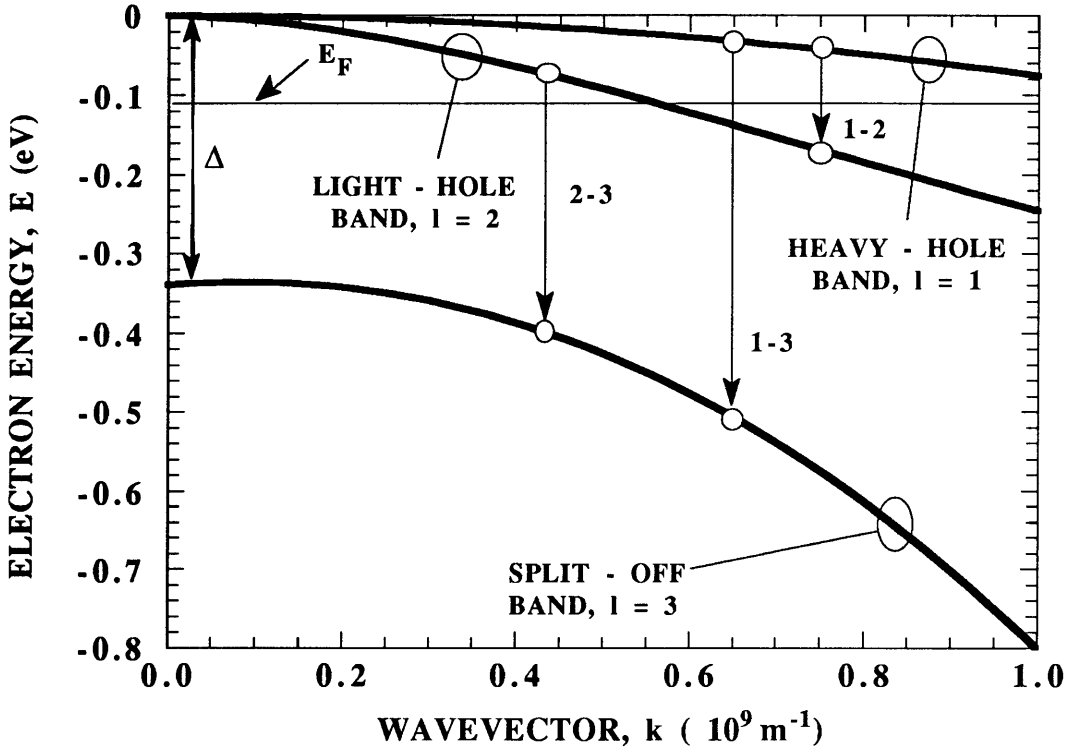

Figure 4-1 Valence subbands of GaAs with direct intersubband transitions. The Fermi energy is for $N_A = 7.0 \times 10^{19}$ cm^{-3}.

energy, where interband transitions dominate the absorption spectrum. To evaluate ε_{isb}, one must determine ω_{ij}, m_{ij}, τ_{ij}, and f_{ij}.

To determine the wavevector-dependent transition frequencies, ω_{ij}, an isotropic model describing the band structure of the valence subbands is required. For GaAs, the heavy-hole band is proportional to k^2, but the other bands are described by more detailed functions. Expressions describing the light-hole band and split-off band are obtained by fitting polynomial functions to the isotropic valence bands calculated by Huberman et al.(1991). The expressions used to calculate the valence band structure shown in Fig. 2-1 and Fig. 4-1 are

$$E_1(k) = -\frac{h_p^2 k^2}{2 m_1} \tag{27}$$

$$E_2(k) = -0.0298 \times 10^{-9} \text{ (eV m)}\, k - 0.464 \times 10^{-18} \text{ (eV m}^2\text{)}\, k^2 + 0.304 \times 10^{-27} \text{ (eV m}^3\text{)}\, k^3 - 0.0657 \times 10^{-36} \text{ (eV m}^4\text{)}\, k^4 \tag{28}$$

$$E_3(k) = -\Delta + 0.0871 \times 10^{-9} \text{ (eV m)}\, k - 0.476 \times 10^{-18} \text{ (eV m}^2\text{)}\, k^2 + 0.0913 \times 10^{-27} \text{ (eV m}^3\text{)}\, k^3 - 0.0196 \times 10^{-36} \text{ (eV m}^4\text{)}\, k^4 \tag{29}$$

where m_1 is the dynamic effective mass of holes in the heavy-hole band, and $\Delta = 0.34$ eV is the spin-orbit splitting energy of GaAs (Blakemore, 1983), shown in Fig. 4-1.

The wavevector-dependent average effective mass, m_{ij}, can be calculated by using Eqs. (3) and (17). In the present work, m_{ij} is assumed to be independent of k, and is calculated using the effective masses at $k = 0$. The effective masses of the holes at $k = 0$ for the heavy-hole, light-hole, and split-off bands for GaAs are $m_1 = 0.5\, m_o$, $m_2 = 0.088\, m_o$, and $m_3 = 0.154\, m_o$, respectively (Blakemore, 1983). The assumption of a k-independent average effective mass can be relaxed if the effective masses of band i or band j vary drastically with k.

The *a priori* determination of the intersubband relaxation time, τ_{ij}, is difficult (Hodgson, 1970). Huberman et al.(1991) and Kaneto et al. (1992) assumed that τ_{12} for GaAs is independent of wavevector, and is approximately equal to the free-carrier relaxation time, τ_{fc}. In the present work, the intersubband relaxation time is assumed to be independent of wavevector, and it is treated as an adjustable parameter.

The calculation of the oscillator strength, f_{ij}, requires the knowledge of the occupation probabilities and the momentum matrix element for each transition. To calculation the momentum matrix element, the wave functions of the initial and final states of each transition must be determined. It is commonly assumed that the momentum matrix elements for transitions between the valence and conduction band are independent of wavevector (Datta, 1989). Brust et al. (1962) confirmed this assumption for interband transitions in Ge by performing detailed calculations of the matrix elements. In the present work, this assumption is extended to intersubband transitions. The square of the magnitude of the momentum matrix element, $| M_{ij}(k) |^2$, is assumed to be independent of wavevector and it is treated as an adjustable parameter.

To calculate the occupation probabilities of the initial and final states of each transition, the Fermi energy must be determined. Equations (4) through (7) provide the Fermi energy of a semiconductor, assuming that N_A, N_V, and T are known. For GaAs, $N_V = 9.52 \times 10^{18}$ cm^{-3} at 300 K (Pierret, 1987). In Fig. 4-1, the Fermi energy for $N_A = 7.0 \times 10^{19}$ cm^{-3} and $T = 300$ K is shown. To determine the occupation probabilities of the initial and final states, the energies of the states are calculated using Eqs. (27) through (29), and are substituted in Eq. (9).

Considering these simplifying assumptions and substituting Eqs. (23), (25), and

(26) into Eq. (22), the dielectric function for p-type semiconductors becomes

$$\varepsilon(\omega) = \varepsilon_{\infty} - \frac{\frac{N_A e^2}{m_1 \varepsilon_o}}{\omega^2 + i \frac{\omega}{\tau_{fc}}} + \frac{\varepsilon_{\infty}[(\omega_L)^2 - (\omega_T)^2]}{(\omega_T)^2 - \omega^2 - i \gamma_{ph} \omega}$$

$$+ \sum_{\substack{ij=12 \\ ij=13 \\ ij=23}} \int_0^{\infty} \frac{2 C_{ij}}{m_{ij} h_p \omega_{ij}(k)} \frac{k^2}{\pi^2} \frac{e^2}{m_{ij} \varepsilon_o} \frac{p_h[E_i(k)] - p_h[E_j(k)]}{\omega_{ij}^2(k) - \omega^2 - i \frac{\omega}{\tau_{ij}}} dk \qquad (30)$$

where $C_{ij} = |M_{ij}|^2$ is the square of the magnitude of the momentum matrix element.

5. EXPERIMENTAL INVESTIGATION FOR P-TYPE GaAs

5.1 Measurements

The samples used in this study consist of beryllium-doped p-type GaAs films on undoped GaAs substrates. Each sample is characterized by the substrate thickness, d_s, the film thickness, d_f, and the dopant concentration of the film, N_A. These parameters are given for each of seven samples in Table 5-1. The samples were fabricated at Raytheon Company (Lexington, MA) by molecular beam epitaxy. The processing conditions and characterization methods for similar samples fabricated at Raytheon Company were described by Hoke et al. (1992). The uncertainty in the dopant concentration is ± 10 percent, the uncertainty in the film thickness is ± 5 percent, and the uncertainty in substrate thickness is ± 2 μm. The samples range in size from 9 mm x 12 mm to 18 mm x 14 mm.

The near-normal reflectance and transmittance of each sample is measured in the spectral range from 1 to 25 μm at room temperature using a Biorad FTS-60A FT-IR spectrometer, with the source beam incident on the film side of the samples. Zhang et al. (1992) gave a detailed description of the experimental system. The reflectance of a gold mirror, 12 mm x 12 mm, is used as a reference for the reflectance measurements. The reflectance of gold at 10 degrees off-normal for the mid-infrared spectral region is 0.98 (Malone et al., 1992), which is used as a correction factor for the raw reflectance data. For the transmittance measurements, the samples are tilted approximately 7 degrees to the normal to reduce multiple reflections. The tilting of the samples reduces the transmittance by approximately 0.5 percent.

Two configurations of source, detector and beamsplitter are used for the measurements. The near-infrared (near-IR) configuration consists of a tungsten-halogen

Table 5-1 Specifications for samples consisting of p-type GaAs films on undoped GaAs substrates. The spectral-overlap offset for each sample is also given.

SAMPLE	d_f (μm)	d_S (μm)	N_A (cm^{-3})	τ_{fc} (s)	E_F (eV)	ΔR_{off} (%)	ΔA_{off} (%)
1	1.0	628	8.0×10^{17}	4.08×10^{-14}	+ 0.0632	- 1.8	2.0
2	0.75	668	5.1×10^{18}	2.90×10^{-14}	+ 0.0112	- 1.9	2.1
3	1.0	639	1.5×10^{19}	2.82×10^{-14}	- 0.0258	- 1.7	2.6
4	0.5	607	2.8×10^{19}	2.50×10^{-14}	- 0.0537	- 1.4	0.9
5	0.5	641	4.5×10^{19}	2.05×10^{-14}	- 0.0809	- 1.2	2.6
6	0.5	584	7.0×10^{19}	1.85×10^{-14}	- 0.1132	- 0.5	0.9
7	0.5	646	1.0×10^{20}	1.71×10^{-14}	- 0.1460	- 0.7	1.4

source, quartz beamsplitter, and PbSe detector, for measurements in the spectral range from 1.0 to 3.0 μm. The mid-infrared (mid-IR) configuration consists of a ceramic source, KBr beamsplitter, and a deuterated triglycine sulfate (DTGS) detector, for measurements in the spectral range 2.5 to 25 μm. For the near-IR measurements, the resolution is 8 cm^{-1}, the aperture setting is 1 cm^{-1}, and 512 scans are averaged for each measurement. For the mid-IR measurements, the resolution is 4 cm^{-1}, the aperture setting is 2 cm^{-1}, and 256 scans are averaged for each measurement.

The photometric accuracy of the measurements is estimated as ± 2 percent. The reflectance and transmittance of an undoped GaAs substrate are measured for the near- and mid-IR spectral ranges. The reflectance and transmittance are calculated by geometric optics (Siegel and Howell, 1981) using the optical constants of undoped GaAs found in the literature (Palik, 1985), and compared with the measured data. The measured reflectance, after being corrected for the non-unity reflectance of the gold mirror, agrees with the calculated reflectance within ± 1.5 percent for all wavelengths in the mid-IR. The measured transmittance agrees with the calculated transmittance within ± 1.5 percent for wavelengths between 2.5 and 19 μm, and within ± 7 percent for wavelengths between 19 and 25 μm, in the region of optical phonon absorption. The agreement in the overlap region between the mid- and near-IR spectral regions is better than 2 percent for both reflectance and transmittance.

The absorptance of the each film-substrate composite sample is calculated by $A_{fs} = 1 - R_{fs} - T_{fs}$, where R_{fs} is the measured reflectance after the gold mirror correction, and T_{fs} is the measured transmittance. The uncertainty in the absorptance is estimated to be ± 2.8 percent, determined by a standard calculation of the propagation of errors (Dally et al., 1984). The measured reflectance and absorptance spectra between 1.0 and 2.5 μm are increased by ΔR_{off} and ΔA_{off} such that the near-IR measurements and mid-IR measurements agree at a wavelength of 2.5 μm. The spectral-overlap corrections are given for each sample in Table 5-1. Discontinuities in the spectra are caused by experimental

errors, so performing the fitting with these discontinuities present would yield physically meaningless parameters.

5.2 Analysis

The values used for the background dielectric constant and phonon parameters of the dielectric function are given in the Section 4.1. The intrasubband relaxation time for each sample is determined from room-temperature mobility measurements performed at Raytheon Company. For the samples 1 through 7, the room-temperature mobilities are 143, 102, 99, 88, 72, 65, and 60 cm^2/Vs, respectively. The intrasubband relaxation times calculated using Eq. (24) are found in Table 5-1. The parameters C_{12}, τ_{12}, C_{13}, and τ_{13} in Eq. (30) are treated as adjustable parameters. The effect of transitions from the light-hole band to the split-off band has been observed for p-type GaAs (Fan, 1967), but for the thin-film samples used in this study, the effect of these transitions is not observed in the measured spectra. Therefore, it is assumed that $C_{23} = 0$. The integral in Eq. (30) is evaluated numerically, with the number of intervals being increased until the calculated absorptance of the sample changes by less than 0.1 percent.

For each sample, the reflectance and transmittance for light incident on the film side are calculated using the method employed by Choi et al. (1992b). Since the film thicknesses are on the order of the wavelength of light in the infrared spectral region, the effects of interference are accounted for using thin-film optics (Yeh, 1988). Since the substrate thicknesses are much larger than the wavelengths of light being considered, geometric optics is employed in the substrate (Siegel and Howell, 1981). The optical constants of the film, n_f and κ_f, and the optical constants of the substrate, n_s and κ_s, are required to calculate the reflectance and transmittance. The optical constants of the substrate are obtained from measured data found in the literature for undoped GaAs

(Palik, 1985). The dielectric function for the film is determined by evaluation of Eq. (30) and the optical constants are determined from Eq. (22).

The best-fit parameters are found by minimization of the chi-squared merit function, χ^2, using the Levenberg-Marquardt method (Press et al., 1986). The inputs to this fitting routine are the measured data points, the standard deviation of the uncertainty in the measured data, the model function to be evaluated, and the parameters in the model function which are to be adjusted to accomplish the best fit. The outputs of the program are the values of the best-fit parameters, the uncertainty in these parameters, and the value of the minimized χ^2.

The absorptance of each sample is used to find the best-fit values of the adjustable parameters because it is more sensitive than reflectance or transmittance to the effects of intersubband transitions. In the region of intersubband absorption, generally between 1.5 and 10 μm, the reflectance is reduced because the film becomes absorbing and the effects of multiple reflections are reduced. The increased absorption in the film also reduces the transmittance. Both of these effects increase the absorptance in this spectral region. In the fitting routine, it is assumed that the standard deviation of the uncertainty is 0.028.

6. RESULTS AND DISCUSSION

The best-fit parameters and associated uncertainties for all samples are given in Table 6-1. The adjustable parameters C_{12} and C_{13} are normalized by dividing by the free-electron mass, m_o, and the spin-orbit splitting energy of GaAs, Δ. All of the parameters and associated uncertainties are the direct results of the fitting routine, except for the parameter τ_{13}. The uncertainties of the parameters C_{12}, τ_{12}, and C_{13} returned by the fitting routine are interpreted as the uncertainties with a 95 percent confidence interval, assuming that the errors in the measured data points are independent and have a normal distribution (Press et al., 1985). These assumptions may not apply rigorously to the data collected with the FT-IR spectrometer, but the uncertainties given in the Table 6-1 are assumed to be reasonable approximations to the true uncertainties. The effect of the uncertainties of other fixed parameters such as d_f, d_s, N_A, and τ_{fc} are not considered, so the magnitudes of the true uncertainties are probably underestimated.

For the parameter τ_{13}, it was observed that the best-fit value yielded by the fitting routine did not capture the shape of the measured absorptance spectra in the spectral region from 1.5 to 4.0 μm. With all other adjustable parameters fixed at their best-fit values, τ_{13} was adjusted until the fitted absorptance resembled the shape of the measured absorptance, with the condition that the magnitude of the fitted absorptance did not differ from the measured absorptance by more than 4 percent. The uncertainties in τ_{23} shown in Table 6-1 were subjectively determined through this fitting-by-eye. Since the uncertainties of the parameters C_{12} , τ_{12}, and C_{13} have a significant effect on the absorptance in the region from 1.5 to 3.5 μm, the uncertainties of τ_{13} are probably underestimated. The uncertainties of all the parameters could be reduced by using samples with larger film thicknesses, as the effect of the intersubband transitions on the absorption spectrum would be stronger. This may also allow the determination of C_{23} and τ_{23}.

Table 6-1 Best-fit parameters for the p-type GaAs samples described in Table 5-1.

SAMPLE	N_A (cm^{-3})	$\frac{C_{12}}{m_o \Delta}$	$\frac{C_{13}}{m_o \Delta}$	τ_{12} (10^{-15} s)	τ_{13} (10^{-15} s)
1	8.0×10^{17}	0.0562 ± 0.0241	0.408 ± 0.602	6.13 ± 5.10	3.0 ± 1.0
2	5.1×10^{18}	0.0359 ± 0.0076	0.277 ± 0.313	9.82 ± 5.10	2.5 ± 1.0
3	1.5×10^{19}	0.0368 ± 0.0029	0.204 ± 0.105	8.98 ± 1.98	2.5 ± 1.0
4	2.8×10^{19}	0.0388 ± 0.0041	0.145 ± 0.093	7.81 ± 1.86	4.0 ± 1.0
5	4.5×10^{19}	0.0420 ± 0.0041	0.181 ± 0.084	7.24 ± 1.52	3.5 ± 1.0
6	7.0×10^{19}	0.0426 ± 0.0035	0.174 ± 0.077	5.58 ± 1.24	4.0 ± 2.0
7	1.0×10^{20}	0.0447 ± 0.0041	0.184 ± 0.071	5.29 ± 2.36	3.5 ± 2.0

$C_{23} = 0.0$

The measured and fitted absorptance spectra of samples 2 (5.1×10^{18} cm^{-3}), 4 (2.8×10^{19} cm^{-3}), and 6 (7.0×10^{19} cm^{-3}) are shown in Fig. 6-1, and the those of samples 1 (8.0×10^{17} cm^{-3}), 3 (1.5×10^{19} cm^{-3}), 5 (4.5×10^{19} cm^{-3}), and 7 (1.0×10^{20} cm^{-3}) are shown in Fig. 6-2. The feature in each measured absorptance spectrum between 1.5 and 3.5 μm is due to transitions $ij = 13$. The feature between 4 μm and approximately 10 μm is due to transitions $ij = 12$. These features have also been observed for thin-film p-type GaAs samples by Huberman et al. (1991). Absorption due to transitions $ij = 23$ is not observable in the spectra because the light-hole band is not populated with holes at large wavevectors. The measured absorptance spectra for the samples with $N_A > 10^{19}$ cm^{-3} begin to decrease between 4 and 12 μm due to plasma reflection. Between 15 and 25 μm, all of the absorptance spectra show absorption by optical phonons in the substrate and the film.

The agreement between the measured and fitted absorptance spectra shows that the model for intersubband transitions is quite effective. The greatest disagreement for all of the samples is in the region of absorption by transitions $ij = 13$. The absorption by transitions $ij = 12$ is stronger than that for transitions $ij = 13$, and affects a greater portion of the spectrum. The fitting routine yields a good fit throughout the $ij = 12$ region at the expense of the goodness-of-fit in the $ij = 13$ region.

Figure 6-3 shows the measured reflectance spectra of samples 2 (5.1×10^{18} cm^{-3}), 4 (2.8×10^{19} cm^{-3}), and 6 (7.0×10^{19} cm^{-3}), and the reflectance spectra *calculated* using the best-fit parameters obtained from fitting the absorptance spectra of these samples. The measured and calculated reflectance spectra of samples 1 (8.0×10^{17} cm^{-3}), 3 (1.5×10^{19} cm^{-3}), 5 (4.5×10^{19} cm^{-3}), and 7 (1.0×10^{20} cm^{-3}) are shown in Fig. 6-4. The effect of plasma reflection is evident in the increase of reflectance for the samples with $N_A > 10^{19}$ cm^{-3}. The agreement between the measured and calculated reflectance spectra is encouraging, considering that no parameters were adjusted to fit these spectra. The

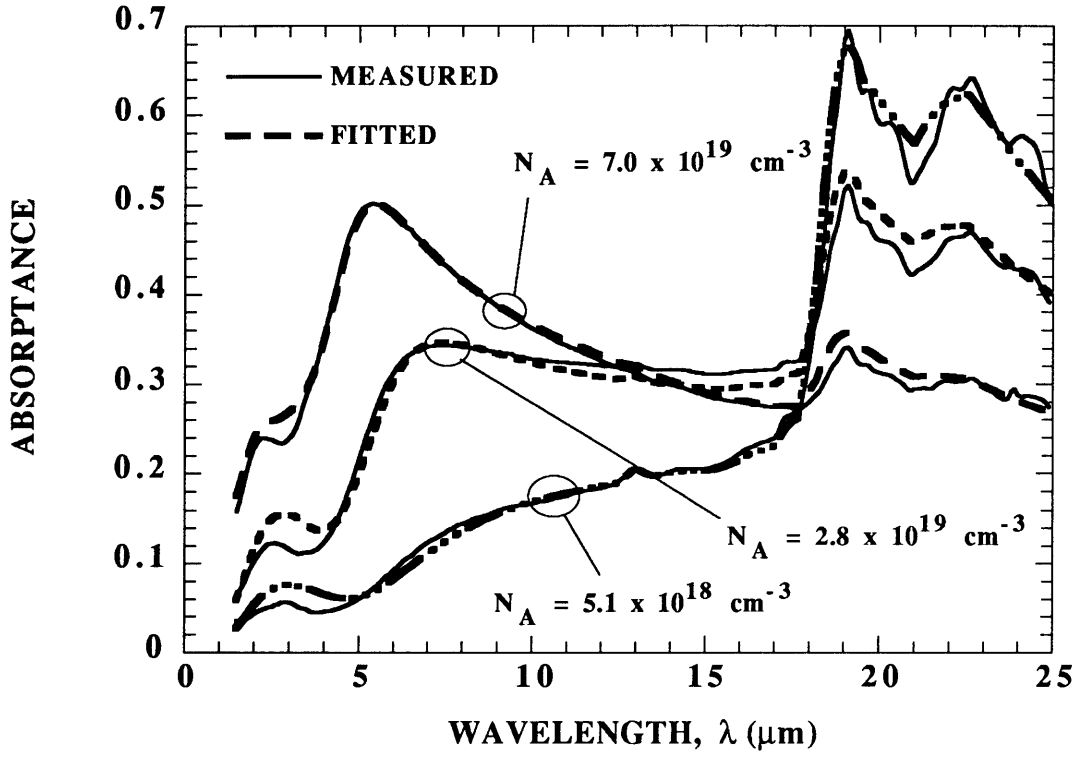

Figure 6-1 Measured and fitted absorptance spectra of samples 2 (N_A = 5.1 x 10^{18} cm^{-3}), 4 (N_A = 2.8 x 10^{19} cm^{-3}), and 6 (N_A = 7.0 x 10^{19} cm^{-3}).

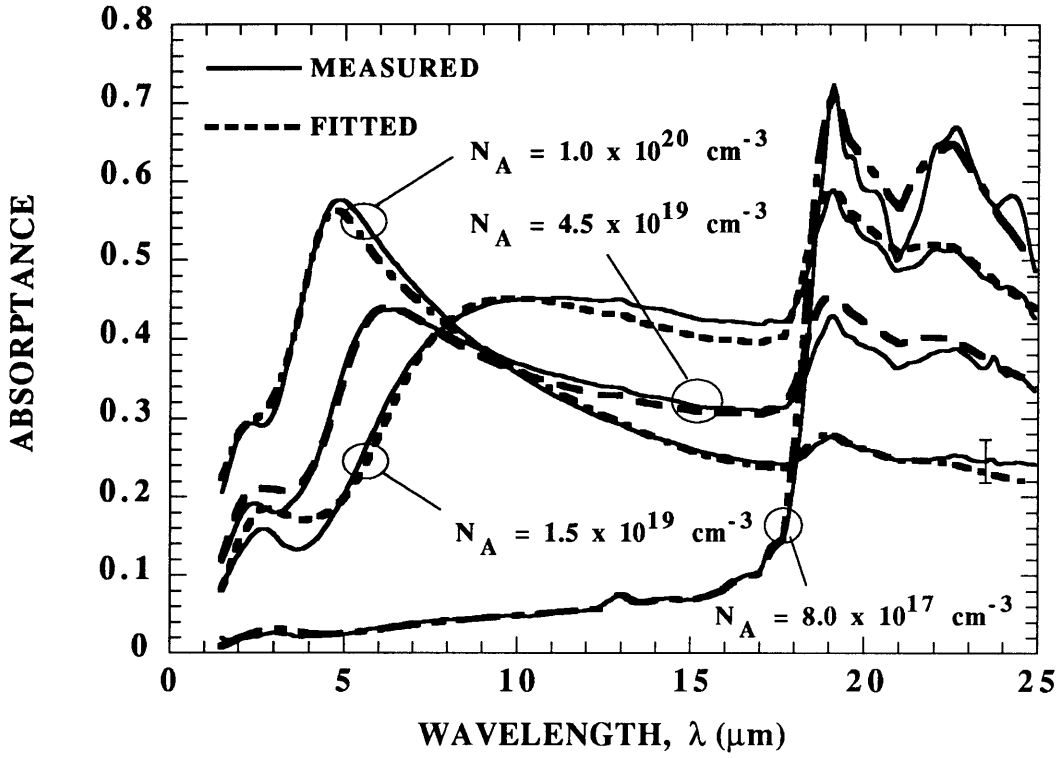

Figure 6-2 Measured and fitted absorptance spectra for samples 1 (N_A = 8.0 x 10^{17} cm^{-3}), 3 (N_A = 1.5 x 10^{19} cm^{-3}), 5 (N_A = 4.5 x 10^{19} cm^{-3}), and 7 (N_A = 1.0 x 10^{20} cm^{-3}).

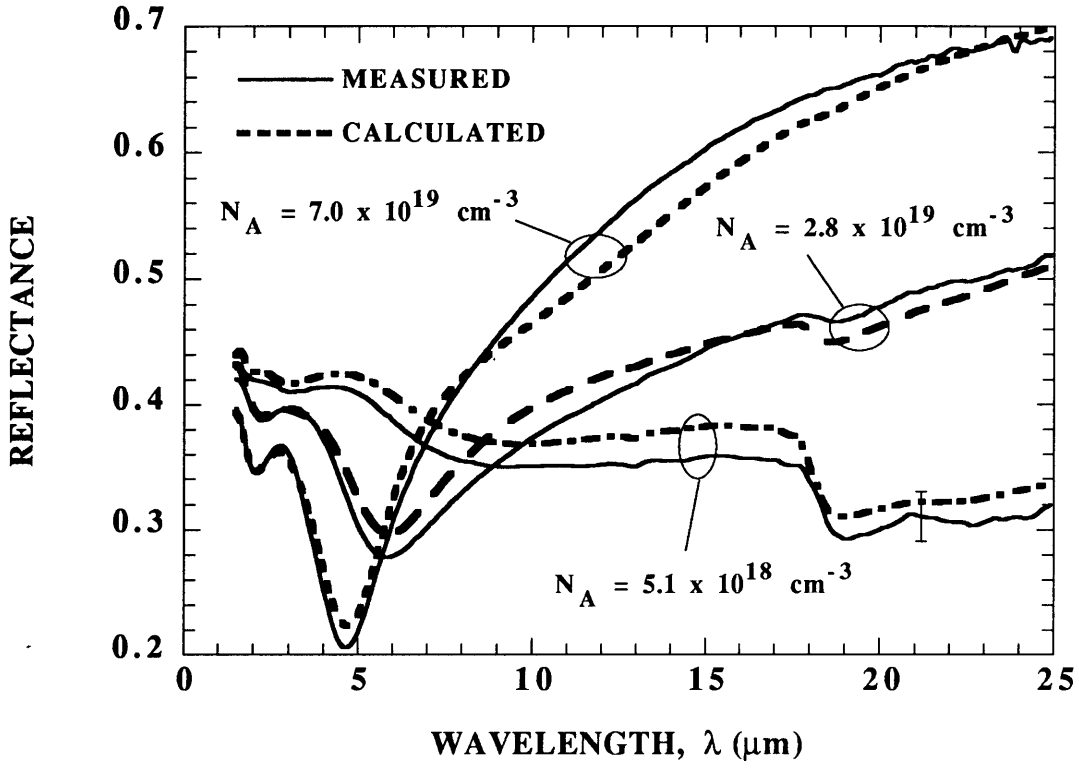

Figure 6-3 Measured and calculated reflectance spectra of samples 2 (N_A = 5.1 x 10^{18} cm^{-3}), 4 (N_A = 2.8 x 10^{19} cm^{-3}), and 6 (N_A = 7.0 x 10^{19} cm^{-3}).

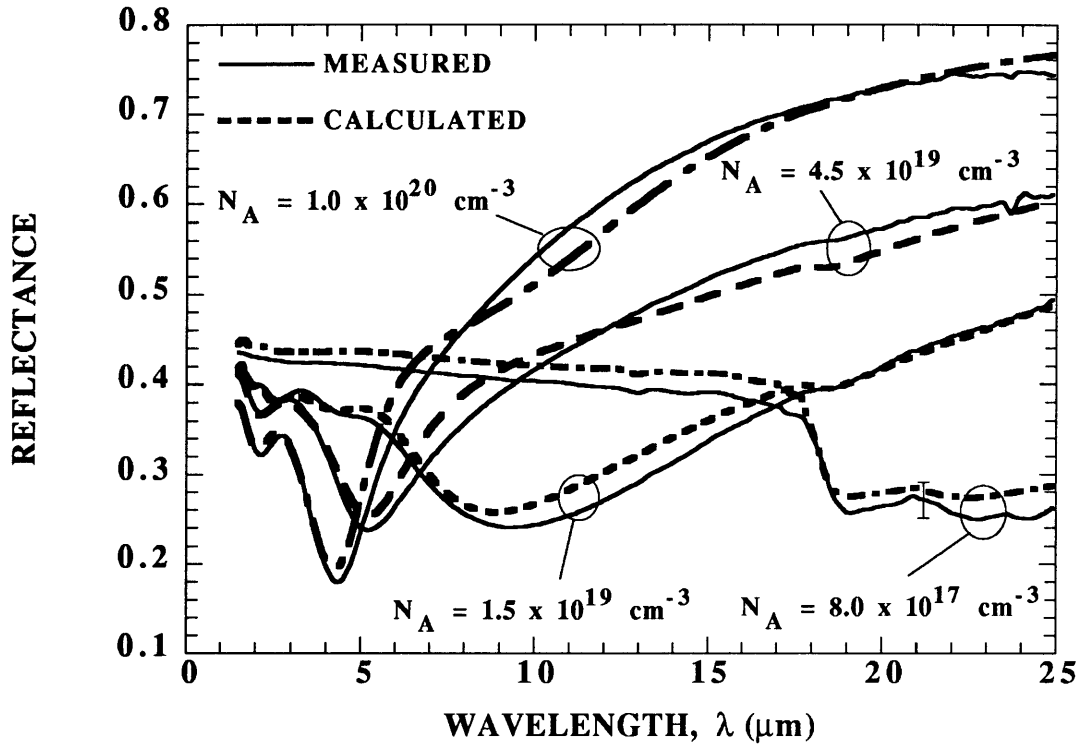

Figure 6-4 Measured and calculated reflectance spectra of samples 1 (N_A = 8.0 x 10^{17} cm^{-3}), 3 (N_A = 1.5 x 10^{19} cm^{-3}), 5 (N_A = 4.5 x 10^{19} cm^{-3}), and 7 (N_A = 1.0 x 10^{20} cm^{-3}).

discrepancies for wavelengths greater than 10 μm are attributed to uncertainties in the dopant concentration and intrasubband relaxation time in the Drude term of the dielectric function.

The refractive index for the dopant concentrations of samples 2 (5.1 x 10^{18} cm^{-3}), 4 (2.8 x 10^{19} cm^{-3}), and 6 (7.0 x 10^{19} cm^{-3}) obtained from the fitting is shown in Fig. 6-5, and the refractive index for samples 1 (8.0 x 10^{17} cm^{-3}), 3 (1.5 x 10^{19} cm^{-3}), 5 (4.5 x 10^{19} cm^{-3}), and 7 (1.0 x 10^{20} cm^{-3}) is shown in Fig. 6-6. The extinction coefficient for the dopant concentrations of these samples is shown in Figs. 6-7 and 6-8. The optical constants of undoped GaAs given by Palik (1985) are shown for comparison. The effect of optical phonons on the optical constants is dominated by free-carrier absorption for all of the dopant concentrations studied in this work, as shown by Fig. 6-7, justifying the assumption of dopant-concentration-independent phonon parameters.

The infrared optical constants obtained in the present work for p-type GaAs with dopant concentrations between 8.0 x 10^{17} and 1.0 x 10^{20} cm^{-3} are more accurate than currently available data. Huberman et al. (1991) calculated the infrared optical constants of p-type GaAs for three dopant concentrations between 2.5 x 10^{19} and 1.5 x 10^{20} cm^{-3}, ignoring the effect of intersubband transitions to the split-off band. The calculated absorptance of thin film samples showed significant disagreement with the measured absorptance, especially in the spectral region from 1.0 to 4.0 μm where the transitions $ij = 13$ contribute to the absorptance. The optical constants in this spectral region are required for the thermal modeling of deposition systems because a significant fraction of blackbody radiation is distributed in this spectral region for typical substrate temperatures.

The importance of accounting for absorption due to intersubband transitions in the dielectric function model is demonstrated in Fig. 6-9, which shows the absorptance spectra for samples 1 (N_A = 8.0 x 10^{17} cm^{-3}) and 7 (N_A = 1.0 x 10^{20} cm^{-3}) calculated by setting $C_{12} = C_{13} = C_{23} = 0$ in Eq. (30). For sample 7 (N_A = 1.0 x 10^{20} cm^{-3}), the error incurred is as large as 40 percent, making it essential to model intersubband transitions. For sample

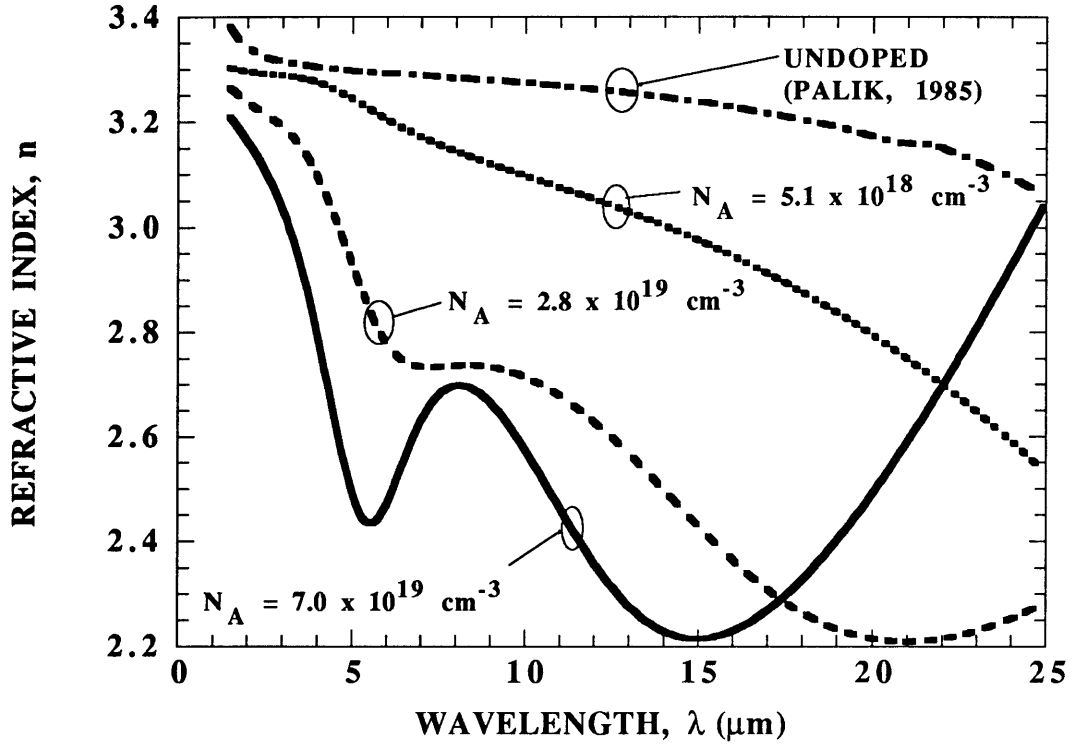

Figure 6-5 Refractive index of undoped GaAs (Palik, 1985) and p-type GaAs with N_A = 5.1 x 10^{18} cm^{-3}, N_A = 2.8 x 10^{19} cm^{-3}, and N_A = 7.0 x 10^{19} cm^{-3} obtained from fitting.

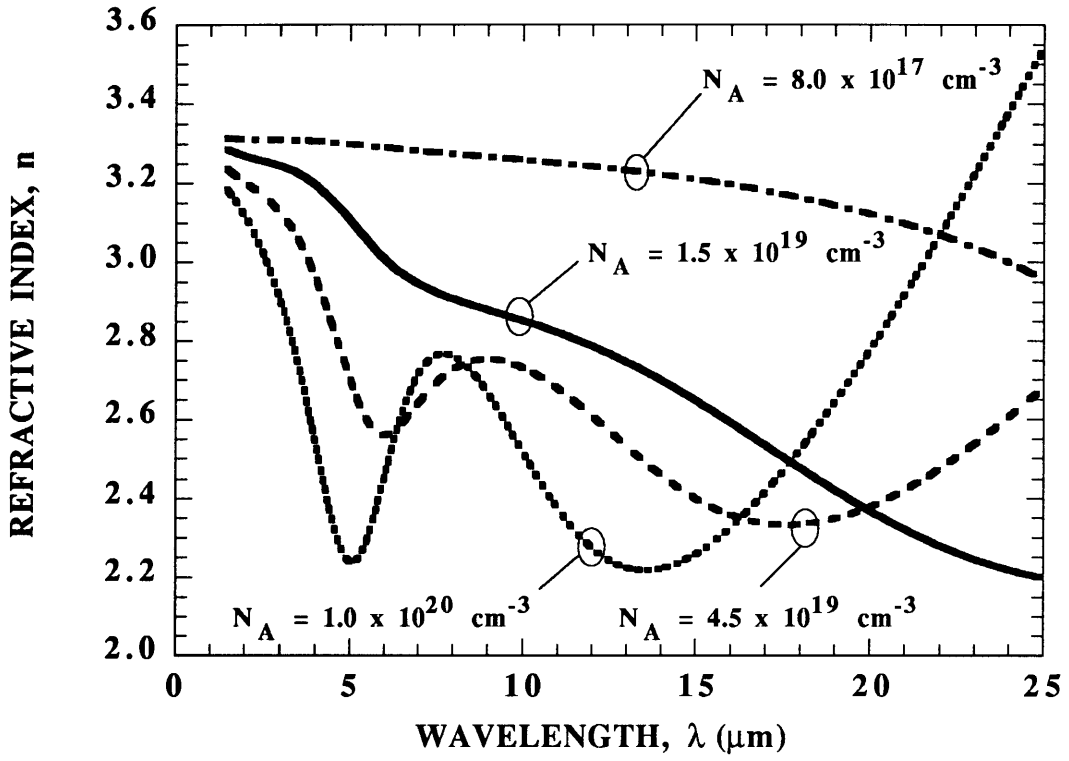

Figure 6-6 Refractive index of p-type GaAs with N_A = 8.0 x 10^{17} cm^{-3}, N_A = 1.5 x 10^{19} cm^{-3}, N_A = 4.5 x 10^{19} cm^{-3}, and N_A = 1.0 x 10^{20} cm^{-3} obtained from fitting.

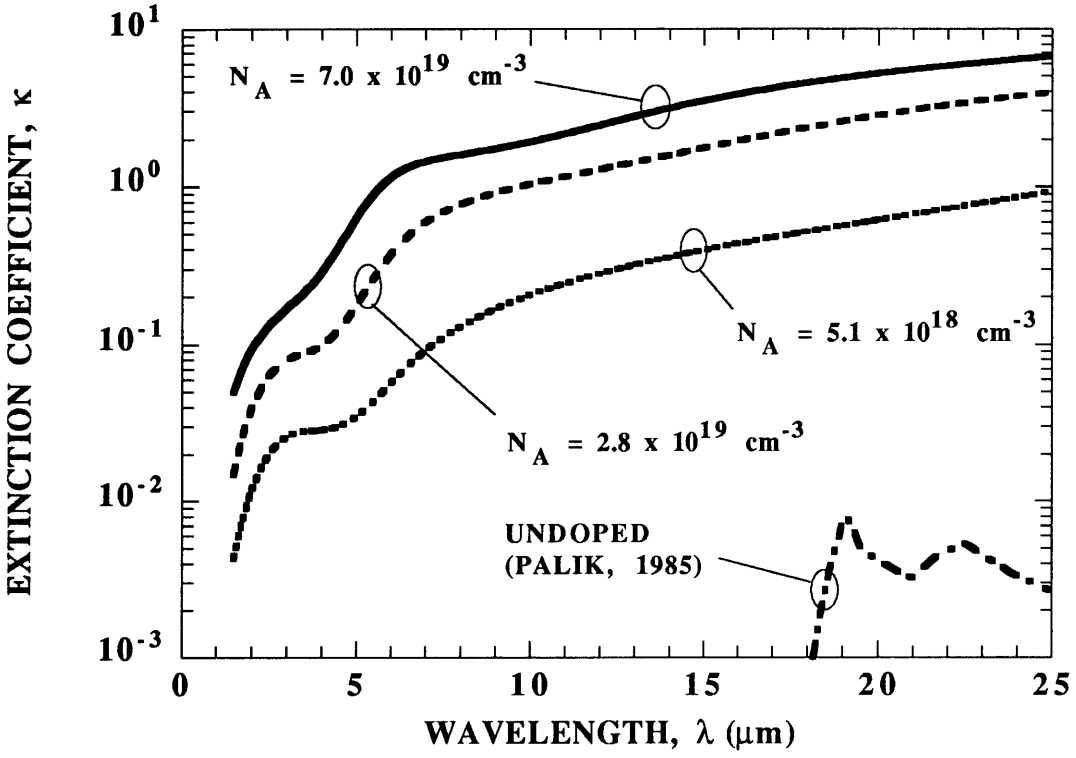

Figure 6-7 Extinction coefficient of undoped GaAs (Palik, 1985) and p-type GaAs with N_A = 5.1 x 10^{18} cm^{-3}, N_A = 2.8 x 10^{19} cm^{-3}, and N_A = 7.0 x 10^{19} cm^{-3} obtained from fitting.

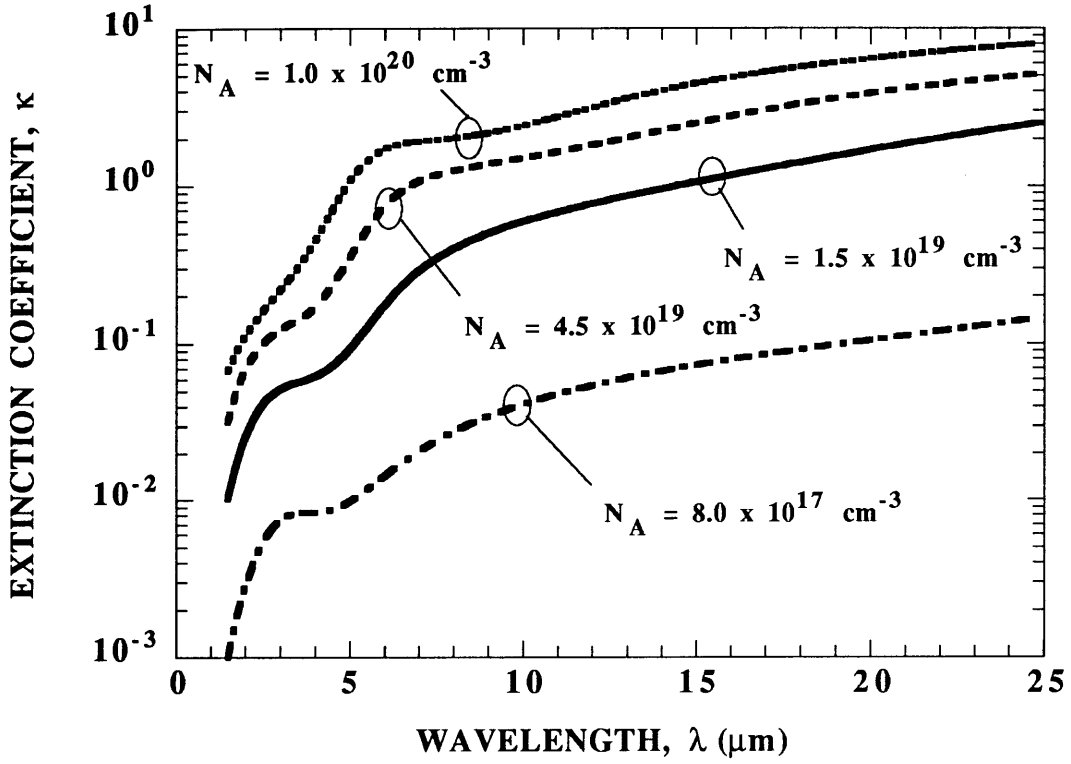

Figure 6-8 Extinction coefficient of p-type GaAs with N_A = 8.0 x 10^{17} cm^{-3}, N_A = 1.5 x 10^{19} cm^{-3}, N_A = 4.5 x 10^{19} cm^{-3}, and N_A = 1.0 x 10^{20} cm^{-3} obtained from fitting.

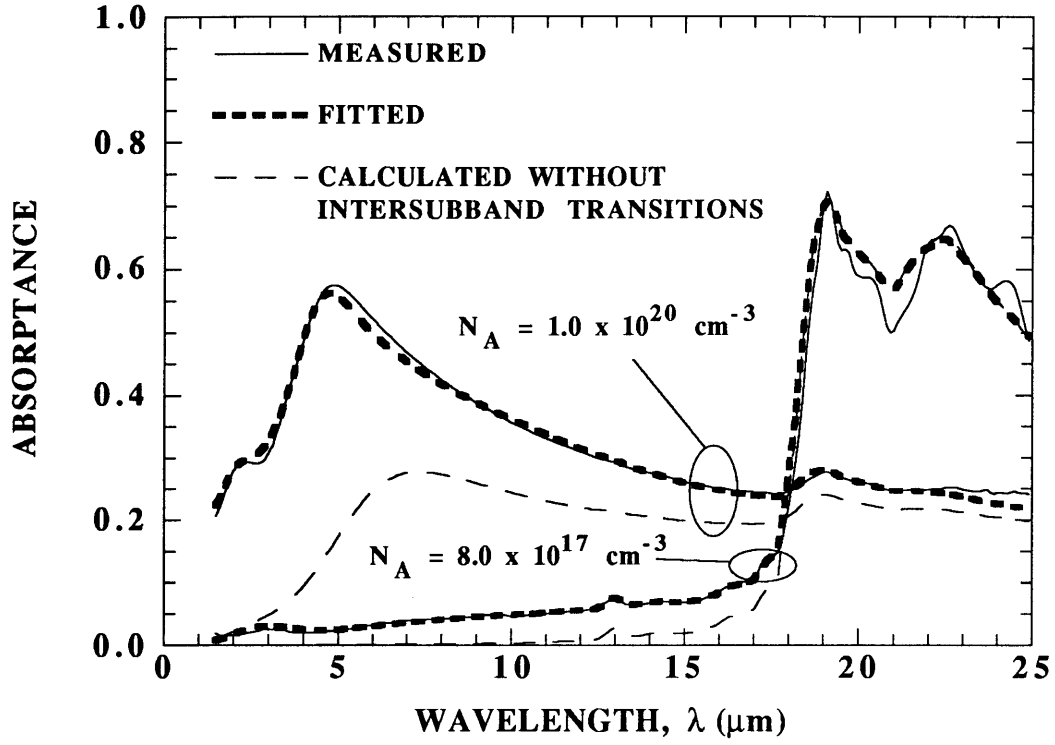

Figure 6-9 Absorptance spectra of samples 1 (N_A = 8.0 x 10^{17} cm^{-3}) and 7 (N_A = 1.0 x 10^{20} cm^{-3}): measured, fitted considering intersubband transitions, and calculated without considering intersubband transitions.

1 (N_A = 8.0 x 10^{17} cm^{-3}), the error is only approximately 5 percent, but the calculation not considering intersubband transitions predicts no absorption for wavelengths less than 10 μm.

The dopant-concentration dependence of the adjustable parameter C_{12} is shown in Fig. 6-10. For the samples with dopant concentrations greater than 5 x 10^{18} cm^{-3}, C_{12} increases with increasing dopant concentration. A curve-fit to the data points with $N_A > 5 \times 10^{18}$ cm^{-3} yields an expression for the recommended value of parameter C_{12},

$$\frac{C_{12}}{m_o \Delta} = 0.0367 + 0.00705 \log\left(\frac{N_A}{N_V}\right) \tag{31}$$

where N_V = 9.52 x 10^{18} cm^{-3} is the effective density of valence band states for GaAs at 300 K (Pierret, 1987). The data point for sample 1 does not follow the same trend as the other samples, and is not included in the fit. There is no apparent reason why the model should not be valid for lower dopant concentrations, and the deviation of this point from the trend requires further investigation. The dopant-concentration dependence of the parameter C_{13} is shown in Fig. 6-11. No trend is apparent, and a dopant-concentration-independent value of C_{13} = 0.18 is recommended. Within the bounds of the error bars associated with C_{13} for the samples with dopant concentrations 8.0 x 10^{17} and 5.1 x 10^{18} cm^{-3}, C_{13} can take on negative values, which is physically meaningless. This emphasizes the need for thicker samples in the experimental investigation to reduce the uncertainties in the adjustable parameters.

The gradual increase in C_{12} with dopant concentration suggests that C_{12} is slowly varying with k, and that the best-fit C_{12} represents an average over the regions in k-space for which transitions ij = 12 occur. Figure 6-12 shows the k-dependence of the oscillator strengths f_{12} and f_{13} for sample 5 (N_A = 4.5 x 10^{19} cm^{-3}), calculated using Eq. (18), except that p_e is replaced by p_h. To applying the sum rule to transitions at a wavevector k, it is assumed that the three valence subbands constitute a three-energy-level system, with

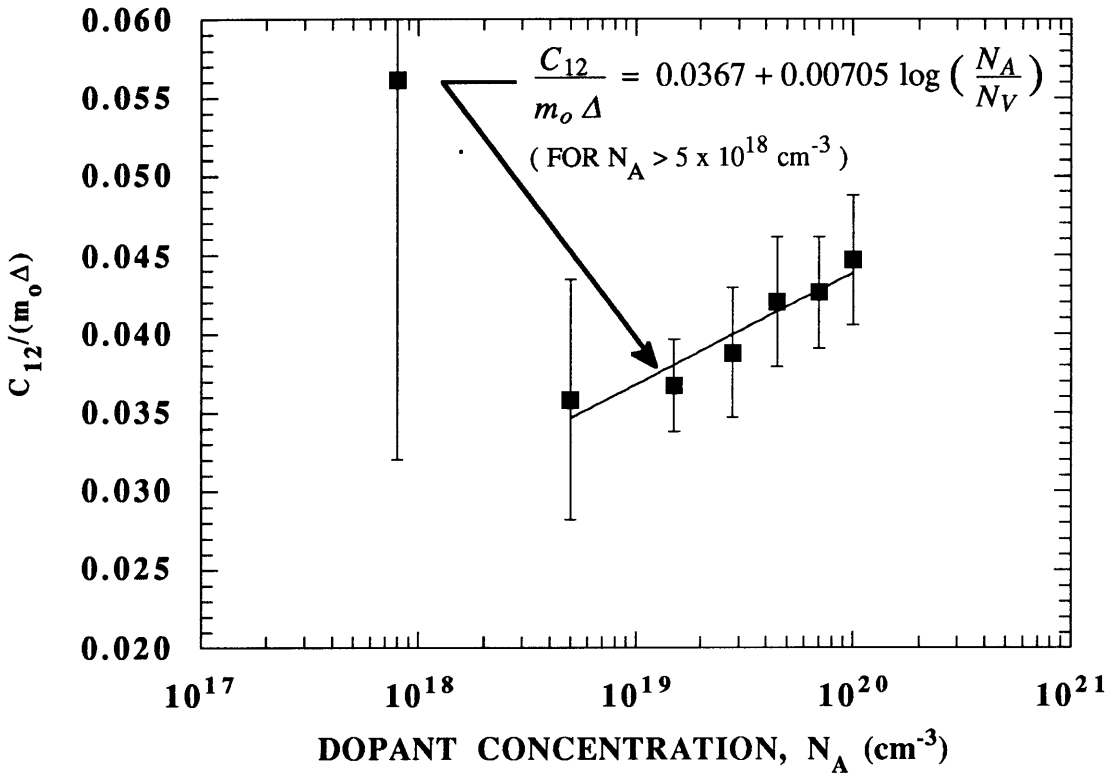

Figure 6-10 Dopant-concentration dependence of the adjustable parameter C_{12}.

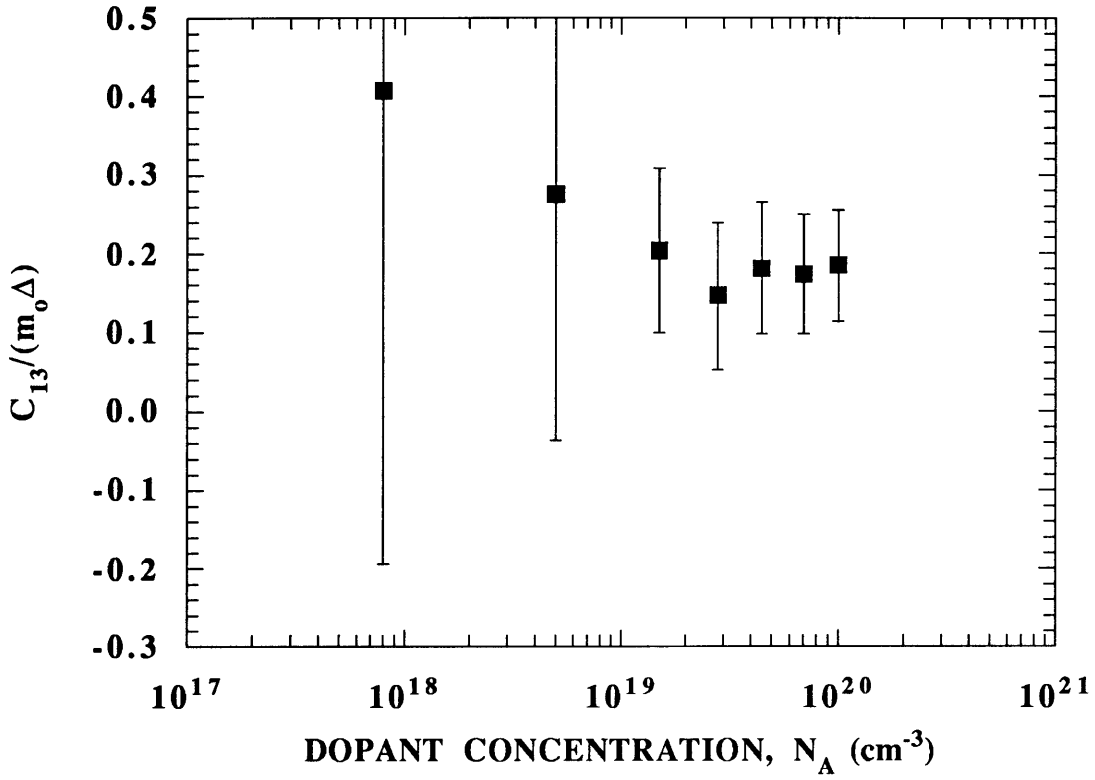

Figure 6-11 Dopant-concentration dependence of the adjustable parameter C_{13}.

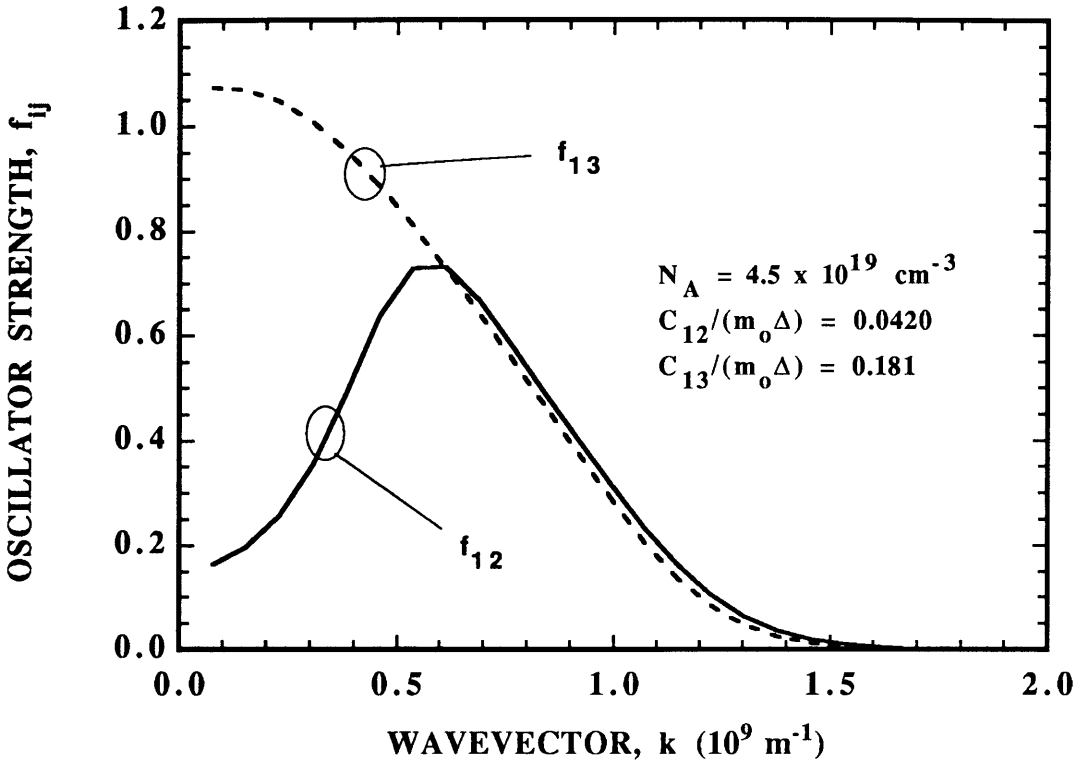

Figure 6-12 Oscillator strengths f_{12} and f_{13} for sample 5 (N_A = 4.5 x 10^{19} cm^{-3}).

$Z = p_h(E_1) + p_h(E_2) + p_h(E_3)$, and $\sum f_{ij} = f_{12} + f_{13} + f_{23}$. Transitions from band 3 do not contribute to the sum of oscillator strengths because the split-off band is not occupied, i.e., $p_h(E_3) \approx 0$. Also, because transitions from band 2 to band 3 are not included in the fitting, f_{23} is unknown. Applying this model to transitions at $k = 0.3 \times 10^9$ m^{-1}, where the bands 1 and 2 are heavily populated with holes, yields $Z = 1.77$, and $f_{12} + f_{13} = 1.36$. Applying the sum rule at $k = 1.5 \times 10^9$ m^{-1}, where bands 1 and 2 are sparsely populated with holes, yields $Z = 0.021$ and $f_{12} + f_{13} = 0.016$. These oscillator strengths are of the correct order of magnitude, and the sum rule is not violated. It is possible that the remaining oscillator strength required to satisfy the sum rule may be accounted for by f_{23}. These calculations suggest that the adjustable parameters C_{ij} have physical significance, but the validity of this approximate application of the sum rule requires further investigation.

The doping dependence of the adjustable parameter τ_{12} is shown in Fig. 6-13. For $N_A > 5 \times 10^{18}$ cm^{-3}, there is trend of a decreasing relaxation time with increasing dopant concentration. The small magnitudes of the uncertainties indicate that the calculated radiative properties are quite sensitive to changes in τ_{12}, emphasizing the importance of accounting for a finite intersubband relaxation time. A curve-fit to the data points for which $N_A > 5 \times 10^{18}$ cm^{-3} yields an expression for the recommended value of parameter τ_{12},

$$\tau_{12} = \left[9.26 - 3.67 \log \left(\frac{N_A}{N_V} \right) \right] \times 10^{-15} \text{ s} \qquad (32)$$

The data point for sample 1 does not follow the same trend as the other samples, and is not included in the fit. The reason for this deviation requires further investigation. The dopant-concentration dependence of the parameter τ_{13} is shown in Fig. 6-14. No trend is apparent and a dopant-concentration-independent value of $\tau_{13} = 3.0 \times 10^{-15}$ s is recommended.

The trends seen in τ_{12} for $N_A > 5 \times 10^{18}$ cm^{-3} suggest that the intersubband relaxation times obtained from the fitting are physically significant. Within the hole gas that

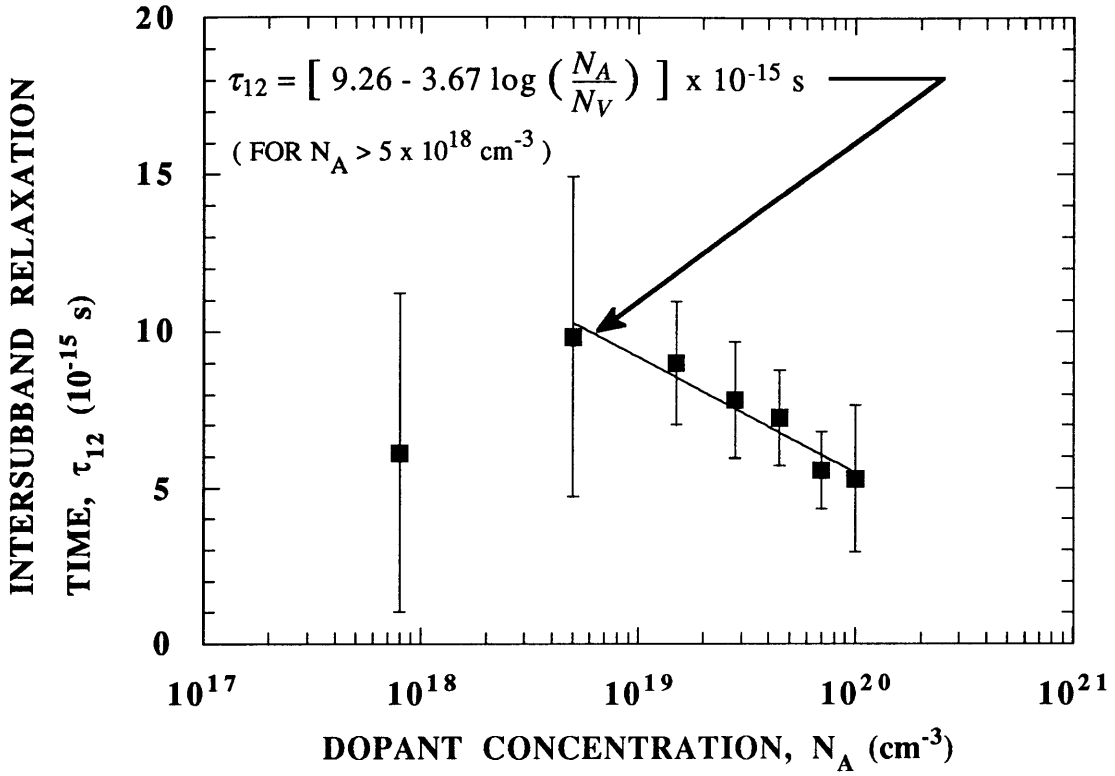

Figure 6-13 Dopant-concentration dependence of the adjustable parameter τ_{12}.

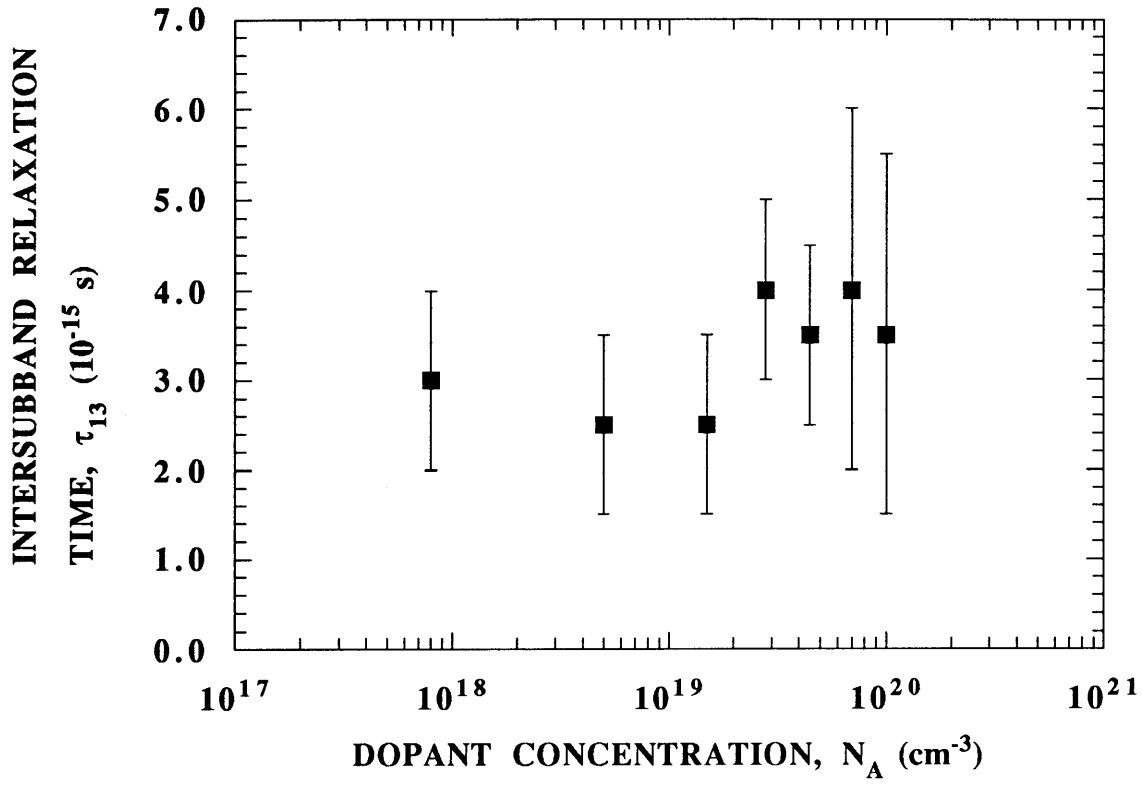

Figure 6-14 Dopant-concentration dependence of the adjustable parameter τ_{13}.

exists in the valence band of a p-type semiconductor, excited holes can relax through collisions with phonons, ionized dopant sites, and other holes. Increasing the dopant concentration increases the density of holes and of ionized dopant sites, both of which tend to decrease the relaxation time of an excited carrier. This trend is also observed for the intrasubband relaxation times obtained from mobility measurements (see Table 6.1). The magnitudes of the intersubband relaxation times τ_{12} shown in Fig. 6-13 are consistent with what has been assumed in the literature. Huberman et al. (1991) and Kaneto et al. (1992) assumed that the intersubband relaxation time for transitions $ij = 12$ in p-type GaAs was approximately equal to the intrasubband relaxation time determined by mobility measurements, which is on the order of 10^{-14} s. The physical mechanisms of intrasubband scattering and intersubband scattering are the same for excited carriers in an electron or hole gas (Appel, 1961), which supports the assumption that $\tau_{12} \approx \tau_{fc}$. However, further investigation is required to determine what scattering mechanisms are dominant for intersubband relaxation, and to explain why the intersubband relaxation times are somewhat less than the intrasubband relaxation times.

In contrast to the more empirical models for interband transitions, the present model requires fewer adjustable parameters and is more flexible. To fit one of the absorptance spectra shown in Figs. 6-1 and 6-2, the method of Verleur (1968) would require 12 adjustable parameters, the method of Forouhi and Bloomer (1992) would require a minimum of 6 adjustable parameters, and the present model requires 4 adjustable parameters. In addition, Eqs. (31) and (32) demonstrate the ability of the model to allow the interpolation of the adjustable parameters between dopant concentrations which have not been experimentally investigated. Adaptation of the model to other semiconductors may be accomplished by using an appropriate isotropic approximation to the band structure. The effects of temperature could also be accounted for through modifications of the band structure and the equilibrium carrier distribution. The temperature dependence of

carrier scattering mechanisms may result in predictable trends in the intersubband relaxation times.

In contrast to the available quantum mechanical methods of predicting radiative properties, the present method is less complicated and yields better agreement with experimental data. Calculation of the transition probabilities from first principles requires the calculation of the wave functions of each electronic state, which is complicated and difficult to achieve with great accuracy. The present approach circumvents this problem by treating C_{ij} as an adjustable parameter, at the expense of ignoring its dependence on wavevector. The finite intersubband relaxation time is either ignored in quantum mechanical approaches (Kane, 1956), or it is assigned some approximate value based on the intrasubband relaxation time (Huberman et al., 1991). The treatment of τ_{ij} as an adjustable parameter seems to be a necessary and practical approach, considering the apparent difficulty of calculating this parameter from first principles (Hodgson, 1970).

7. CONCLUSIONS

1. This study provides a model for absorption due to direct intersubband transitions in doped semiconductors that allows the achievement of quantitative agreement with measured radiative properties.

2. The simplicity of the model makes it useful for engineering calculations, and the trends demonstrated by the adjustable parameters allow the extension of the model to dopant concentrations which have not been experimentally investigated.

3. The dopant-concentration dependence and magnitude of the intersubband relaxation time for transitions from the heavy-hole band to the light-hole band strongly suggest that this parameter has physical significance. The application of the sum rule for oscillator strengths suggests that the adjustable parameters that govern transition probability also have physical significance.

4. The model demonstrates the importance of accounting for a finite intersubband relaxation time in the calculation of radiative properties.

8. RECOMMENDATIONS

1. The validity of the present model for dopant concentrations below 5 x 10^{18} cm^{-3} should be established. This could be accomplished through an experimental investigation of either film-substrate composites with thicker films or doped substrates. The uncertainties in the adjustable parameters for all dopant concentrations would be reduced, and the determination of the adjustable parameters for transitions from the light-hole band to the split-off band may be possible.

2. The physical significance of the adjustable parameters should be explored in more depth. This would facilitate the judging of the validity of results, and the extension of the model to higher temperatures and dopant concentrations which have not been experimentally investigated.

3. The present model should be used to build a library of temperature-dependent infrared semiconductor optical constants. The knowledge of the infrared optical constants of semiconductors at processing temperatures, which are typically between 400 and 700°C, may facilitate *in situ* control of these processes. Thermal modeling of semiconductor deposition processes could facilitate the prediction of undesirable substrate temperature fluctuations (Hoke et al., 1992), and may also be useful for the design of deposition systems. Choi et al. (1993) have investigated the use of FT-IR spectroscopy for *in situ* control of dopant concentration and film composition during deposition processes. Adaptively calibrated pyrometry (Choi et al., 1992a) is a promising method of substrate temperature control in deposition processes. All of these tools require accurate experimental data and simple, accurate models for the infrared optical constants of semiconductors at processing temperatures.

4. The present model should be used for the design of infrared detectors which exploit intersubband transitions. Examples of such detectors are heterojunction internal photoemission detectors (Huberman et al., 1991) and $GaAs/Al_xGa_{1-x}As$ multiple quantum well detectors (Osbourn, 1990). The ability to accurately predict the radiative properties of such detectors would allow the optimization of detector design. The accurate prediction of the radiative properties of multiple quantum wells requires a simple model for the size-effect on semiconductor optical constants, which is another challenge which may benefit from this simple model for absorption due intersubband transitions.

REFERENCES

Appel, J., 1961, "Interband Electron-Electron Scattering and Transport Phenomena in Semiconductors," *Phys. Rev.*, Vol. 122, pp. 1815-1823.

Ashcroft, N.W., and Mermin, N.D., 1976, *Solid State Physics*, W.B. Saunders Company, Philadelphia, Appendices K and M.

Bassani, F., and Parravicini, G.P., 1975, *Electronic States and Optical Transitions in Solids*, Permagon Press Inc., New York, Chapter 5.

Blakemore, J.S., "Semiconducting and Other Major Properties of Gallium Arsenide," 1982, *J. Appl. Phys.*, Vol. 53, pp. R123-R181.

Brust, D., Phillips, J.C., and Bassani, F., 1962, "Critical Points and Ultraviolet Reflectivity of Semiconductors," *Phys. Rev. Letters*, Vol. 9, pp. 94-97.

Choi, B.I., Flik, M.I., and Anderson, A.C., 1992a, "Adaptively Calibrated Pyrometry for Film Deposition Processes," in *Heat Transfer in Materials Processing*, ASME HTD-Vol. 22, J.C. Khanpar and P. Bishop, eds., pp. 19-26.

Choi, B.I., Zhang, Z.M., Flik, M.I., and Siegrist, T., 1992b, "Radiative Properties of Y-Ba-Cu-O Films with Variable Oxygen Content," *Journal of Heat Transfer*, Vol. 114, pp. 958-964.

Choi, B.I., Hebb, J.P., and Flik, M.I., 1993, "Measurement of Composition and Dopant Concentration of Semiconductors Using FT-IR Spectroscopy," accepted to *Sixth International Symposium on Transport Phenomena in Thermal Engineering*, Seoul, Korea, May 9-13, 1993.

Cohen, M.L., and Chelikowsky, J.R., 1989, *Electronic Structure and Optical Properties of Semiconductors*, Springer-Verlag, Berlin, Chapter 8.

Dally, J.W., Riley, W.F., and McConnel, K.G., 1984, *Instrumentation for Engineering Measurements*, John Wiley and Sons, Inc., New York, Chapter 10.

Datta, S., 1989, *Quantum Phenomena*, Addison Wesley Publishing Co., New York, Chapter 7.

Dumke, W.P., 1961, "Quantum Theory of Free Carrier Absorption," *Phys. Rev.*, Vol 124, pp. 1813-1817.

Fan, H.Y., 1967, "Effects of Free Carriers on the Optical Properties," in *Semiconductors and Semimetals*, Vol. 3., R.K Willardson and A.C. Beer, eds., Academic Press, New York.

Forouhi, A.R. and Bloomer, I., 1992, "Calculation of Optical Constants, n and k, in the Interband Region," in *Handbook of Optical Constants II*, E.D. Palik, ed., Academic Press, San Diego.

Garbuny, M., 1965, *Optical Physics*, Academic Press, New York, Chapter 1.

Harrison, W.A., 1980, *Electronic Structure and Properties of Solids*, W.H. Freeman and Company, San Francisco, Chapters 2 and 4.

Hodgson, J.N., 1970, *Optical Absorption and Dispersion in Solids*, Chapman and Hall Ltd., London, Chapter 3.

Hoke, W.E., Weir, D.G., Lemonias, P.J., and Lyman, P.S., 1992, "Enhanced Radiative Absorption of Thin, Heavily Beryllium Doped GaAs Films," *Electronic Materials Conference*, June, 1992, to appear in *Journal of Electronic Materials*.

Huberman, M.L., Ksendzov, A., Larsson, A., Terhune, R., and Maserjian, J., 1991, "Optical Absorption by Free Holes in Heavily Doped GaAs," *Phys. Rev. B*, Vol. 44, pp. 1128-1133.

Kane, E.O., 1956, "Energy Band Structure in p-type Germanium and Silicon," *J. Phys. Chem. Solids*, Vol. 1, pp. 82-99.

Kaneto, T., Kim, K.W., and Littlejohn, M.A., 1992, "Dielectric Response Functions of Heavily Doped Zincblende Semiconductors with Finite Particle Lifetime," *J. Appl. Phys.*, Vol. 72, pp. 4139-4147.

Kittel, C., 1986, *Introduction to Solid State Physics*, John Wiley and Sons, Inc., New York, Chapters 5 and 6.

Malone, C.G., Choi, B.I., Flik, M.I., and Cravalho, E.G., 1992, "Emissivity of Anisotropic Solid Media," *ASME National Heat Transfer Conference*, San Diego, August 9-12, 1992, to appear in *Journal Of Heat Transfer*.

Osbourn, G.C., 1990, "Design of III-V Quantum Well Structures for Long-wavelength Applications," *Semicond. Sci. Technol.*, Vol. 5, pp. S5-S11.

Palik, E.D., 1985, "Gallium Arsenide (GaAs)," in *Handbook of Optical Constants of Solids*, E.D. Palik, ed., Academic Press, New York, pp. 429-443.

Pankove, J.I., 1971, *Optical Processes in Semiconductors*, Dover Publications Ltd., New York, Chapter 3.

Perkowitz, S., 1992, "Infrared Properties of Semiconductors: Talking Physics with Simple Models, a lá Eli Burnstein," *Solid State Communications*, Vol. 84, pp. 19-23.

Pierret, R.F., 1987, *Advanced Semiconductor Fundamentals*, Addison Wesley Publishing Company, Reading, MA, Chapters 3 and 4.

Press, W.H., Flannery, B.P., Teukolsky, S.A., Wetterling, W.T., 1986, *Numerical Recipes*, Cambridge University Press, Cambridge, Chapter 14.

Rode, D.L., 1975, "Low Field Electron Transport," in *Semiconductors and Semimetals*, Vol. 10, R.K. Willardson and A.C. Beer, eds., Academic Press, New York.

Sell, D.D., Casey, H.C., Jr., and Wecht, K.W., 1974, "Concentration Dependence of the Refractive Index for n- and p- type GaAs between 1.2 and 1.8 eV," *J. Appl. Phys.*, Vol. 45, pp. 2650-2657.

Siegel, R., and Howell, J., 1981, *Thermal Radiation Heat Transfer*, Hemisphere Publishing Corporation, New York, Chapter 19.

Stern, F., 1963, "Elementary Theory of the Optical Properties of Solids," in *Solid State Physics*, Vol. 15, F. Seitz and D. Turnbull, eds., Academic Press, New York,.

Verleur, H.W., 1968, "Determination of Optical Constants from Reflectance or Transmittance Measurements on Bulk Crystals or Thin Films," *J. Opt. Soc. Am.*, Vol. 58, pp. 1356-1364.

Wooten, 1972, *Optical Properties of Solids*, Academic Press, New York, Chapter 3.

Yeh, P., 1988, *Optical Waves in Layered Media*, John Wiley and Sons, Inc., New York, Chapter 5.

Zhang, Z.M., Choi, B.I., Le, T.A., Flik, M.I., Siegal, M.P., and Phillips, J.M., 1992, "Infrared Refractive Index of Thin $YBa_2Cu_3O_7$ Superconducting Films," *Journal of Heat Transfer*, Vol. 114, pp. 644-652.